WADC TECHNICAL NOTE 59-307
VOLUME III

# STUDY OF INSTRUMENTATION AND TECHNIQUES FOR MONITORING VEHICLE AND EQUIPMENT ENVIRONMENTS AT HIGH ALTITUDE

## INSTRUMENTATION AND MONITORING TECHNIQUES

B. V. Wacholder and E. Fayer

Radio Corporation of America

June 1960



Flight Control Laboratory

Contract No. AF 33(616)-6407

Project No. 8223

Task No. 82177

WRIGHT AIR DEVELOPMENT DIVISION
Air Research and Development Command
United States Air Force
Wright-Patterson Air Force Base, Ohio

## NOTICES

When Government drawings, specifications, or other data are used for any purpose other than in connection with a definitely related Government procurement operation, the United States Government thereby incurs no responsibility nor any obligation whatsoever; and the fact that the Government may have formulated, furnished, or in any way supplied the said drawings, specifications, or other data, is not to be regarded by implication or otherwise as in any manner licensing the holder or any other person or corporation, or conveying any rights or permission to manufacture, use, or sell any patented invention that may in any way be related thereto.

Qualified requesters may obtain copies of this report from the Armed Services Technical Information Agency, (ASTIA), Arlington Hall Station, Arlington 12, Virginia.

Copies of WADD Technical Reports and Technical Notes should not be returned to the Wright Air Development Division unless return is required by security considerations, contractual obligations, or notice on a specific document.

AF-WP-8-MAY 60 1M

# FOREWORD

This study was initiated by the Flight Control Laboratory, Wright Air Development Division, Wright-Patterson Air Force Base, Ohio. The investigations on which this final report is based were performed under Contract No. AF33(616)-6407. This contract was initiated under Project No. 8223, Crew and Vehicle Environmental Data Sensing and Instrumentation, Task No. 82177, Vehicle Environmental Data Sensing and Instrumentation. Mr. P. Polishuk, of the Flight Control Laboratory, acted as Project Engineer for this work.

The results of this study are presented in three volumes.

Study of Instrumentation and Techniques for Monitoring Vehicle and Equipment Environments at High Altitudes.

Volume I - Vehicles and Environments.

Volume II - Effects of High Altitude Environments on Vehicles and Equipment.

Volume III - Instrumentation and Monitoring Techniques

The authors of the report are B. V. Wacholder and E. Fayer of the Airborne Systems Division, Radio Corporation of America.

The material presented in the final report was made possible through the cooperation of many individuals in industry and in Government Agencies. Those industrial and governmental facilities consulted and listed in appendix B of Volume II of this report.

## ABSTRACT

This Volume III presents instrumentation techniques available within the state-of-the-art, and proposes an instrumentation system for the monitoring of high-altitude environments encountered by typical vehicles.

Section I summarizes the high altitude environmental effects on typical vehicles and equipment and is a concise treatment of the materials contained in Volumes I and II of this final report.

Section II presents the present airborne-instrumentation state-of-the-art for measuring temperature, pressure, strain, vibration, acceleration, radiation, meteorite detection, and acoustic noise.

Sections III and IV discuss a feasible instrumentation system for monitoring these deleterious environments. In addition, recommendations are made for an extension of this study to cover environments that are outside the scope of the present program, such as the environments created by nuclear and other advanced propulsion systems. Another recommendation is the continuation of the instrumentation study to effect a complete design specification for an environmental monitoring system for a particular vehicle.


## PUBLICATION REVIEW

The publication of this report does not constitute approval by the Air Force of the findings or conclusions contained herein. It is published only for the exchange and stimulation of ideas.

FOR THE COMMANDER:

H. W. BASHAM
Chief Control Elements
Research Branch
Flight Control Laboratory
Aeromechanics Division

TABLE OF CONTENTS

TABLE OF CONTENTS (Continued)

TABLE OF CONTENTS (Continued)

## LIST OF ILLUSTRATIONS

LIST OF ILLUSTRATIONS (Continued)

## LIST OF TABLES

## INTRODUCTION

This Technical Note contains the results of a study performed by the Radio Corporation of America and sponsored by the Flight Control Laboratory, Instrumentation Section, Wright Air Development Division, to determine the environments at the fringes of the earth's atmosphere and out to the surface of the moon and their effect on vehicles and equipment. The ultimate objective of this study is to establish design criteria for the development of instrumentation to monitor environments deleterious to the vehicle or equipment. The instrumentation requirements can be established only after a thorough study of the environments and an analysis of the interaction of the environments and the equipment. To accomplish this, the effort was therefore divided into three phases.

During the first phase, data was obtained on the natural and induced environments as they exist in the regions of space of interest to this study. An indication of the severity of these space environments is given below:

Velocity at re-entry: 3.2 to 11.3 KM/sec.

Stagnation temperature: (1650°C to 2200°C)

Pressures in orbit: $10^{-15}$ mm Hg

Solar radiation (unattenuated by atmosphere): 1400 $w/m^2$

Van Allen radiation: Protons with energy up to 100 mev (inner belt)
Electrons with energy up to 1 mev (outer belt)

Solar Winds: Velocities - 1000 meters/second
Radiation intensity - 500 r/hour

These and other environments, such as dissociated and ionized gases, constitute the operational regime of the future space craft.

During the second phase an analysis was made to determine the effect of the environments on typical vehicles and equipment based on the environmental data and on a knowledge of materials and equipment in high altitude vehicles. The results of this phase are summarized in Figure 1A, Volume II.

During the third phase, the instrumentation techniques suitable for monitoring high-altitude environments and possible deleterious effects were examined to establish the instrumentation requirements.

Flight vehicles have tended towards more automation and instrumentation as their speed has increased. These instruments compensate for the limitations of response to the human operator. It is safe, therefore, to assume that

elaborate instrumentation will be required to cope with these new space environments. Instrumentation to date has been mostly to aid the pilot in his navigation, guidance, and control tasks with only a minimal amount devoted to safety.

The problem of monitoring instrumentation in space vehicles has been examined thoroughly. Monitoring instrumentation may seem redundant to good design; that is, the question might be asked, why use instruments to monitor the environments; why not design for it? However, in view of the somewhat meager knowledge of this novel environment and its effects on the vehicle, and in addition the complete helplessness of the pilot in empty space in the event of failure, this "redundancy" of monitoring instrumentation is justified.

The three phases of the program comprise the three volumes of this final report. This Volume III presents design criteria for space instrumentation. Instruments capable of monitoring such parameters as temperature, pressure, and radiation are examined for their suitability for the application. The study of the state of the art is first reviewed; desirable developments are indicated where suitable instrumentation does not exist.

A prime consideration is the unification of the instrumentation into a complete system rather than a collection of parts, which has frequently been the case in aircraft development. Another consideration is the relation of the monitor instrumentation to the Flight Control instrumentation. The study of the Flight Control requirements for high-altitude vehicles was made by Bell Aircraft under contract with WADD. It may be possible to use the same intelligence source or transducer for both safety and control, thereby avoiding duplication.

## SECTION I

## SUMMARY OF ENVIRONMENTAL EFFECTS

Volumes I and II of this study program have established the need for in-flight instrumentation to continuously monitor hazardous environments. Only after a thorough analysis of the environments and vehicle interaction can this be accomplished. The following summary of hazardous effects of the environments on the vehicles provides justification for the instrumentation.

By far the most deleterious environment which a vehicle can encounter is the aerodynamic heating generated by a hypersonic re-entry into a planetary atmosphere. The heating rate is a function of vehicle speed, re-entry angle, lift-to-drag ratio, and atmospheric density. Normal heating rates for the various types of re-entry profiles vary from 20 to 100 BTU/$ft^2$-sec for a glide vehicle at varying angle of entry to 500 to 5000 BTU/$ft^2$-sec for a ballistic re-entry at an angle of entry varying from 10 to 90 degrees from the horizontal. Glide re-entry stagnation temperatures are expected to be in the range of 3000 degrees F, which has been chosen as the working value for the proposed instrumentation. The need for temperature instrumentation is justified by the fact that any variation in the vehicle flight parameters could lead to excessive heat rates which go beyond the design limits of the vehicle and become hazardous. Heat transfer to the interior of the vehicle because of excessive heat rates could cause malfunction of electronic equipment causing system failure. Effects of temperature on systems have been discussed in detail in Volume II of this study. Structural failure due to excessive heat loads and high dynamic pressures is the immediate hazard. (This, in conjunction with the structural strain caused by the dynamic loading, warrants the need for structural strain measurements.)

Another problem area to contend with during hypersonic re-entry is the dynamic pressure loading the vehicle will experience. The dynamic pressure is a function of the vehicle speed, the atmospheric density, and the ratio of gravitational to aerodynamic forces (lift-to-drag ratio). Expected maximum dynamic pressures to be encountered during hypersonic re-entry are in the range of 2500 to 6000 psf (the former for the X-15 aircraft, the latter for Dyna-Soar). Exceeding the design limits for dynamic pressure could lead to surface panel buckling and overstressed structural members. A study of the dynamic pressure effects are presented in detail in Volume II of this study.

Manuscript released by the authors June 1960 as a WADC Technical Note.

Aside from the two extremely hazardous re-entry environments presented above, there exist several less hazardous ones which may be encountered during boost and re-entry. They are aerodynamic noise, vibration and acceleration. During boost, noise from the power plant will be as high as 150 db at the manned vehicle. Aerodynamic noise will be about the same magnitude during re-entry. Without proper acoustic shielding and damping, noise induced vibrations can lead to serious structural fatigue which can cause cracks in the structural surface or failure of structural members. Transmissibility into the vehicle interior could cause damage to sensitive instruments and to the pilot. These effects warrant the monitoring of aerodynamically induced acoustic and powerplant vibration during re-entry and boost phases.

Accelerations during the boost phase are dependent upon the thrust buildup of the booster engines. Excessive accelerations could overstress structural members and be damaging to sensitive instruments and the pilot. Acceleration monitoring during the boost phase could be utilized for thrust control. Accelerations during boost are expected to be about 9 g. Re-entry accelerations for a glide vehicle at a shallow angle of re-entry will be about 1 to 2 g. However, entering at too steep an angle can lead to high g levels. A ballistic re-entry, angle of re-entry about 90 degrees, can lead to g levels around 60 g. It is obvious what occurs if a glide vehicle designed for a shallow re-entry enters at too steep an angle. Excessive heating, pressure loading, and acceleration will cause destruction of the vehicle. (A means of continuously monitoring acceleration during re-entry is essential to vehicle safety.)

The application of a hypersonic glider to space travel will impose several natural environments upon the vehicle which could be hazardous to the vehicle safety. These are the particle radiation of solar origin, the micro-meteorite particles existing in free space, and continuous high vacuum.

The major problem presented by the radiation surrounding the earth (see Volume I) is the shielding required to protect the pilot and equipment aboard. The parameters of concern here are the length of exposure and the total integrated effect. At present the highest dosage to be anticipated during normal solar activity is 10r/hr. Anticipated structural damage could be accounted for in design; however, excessive radiation dosages (500 to 1000r/hr during violent solar activity) will have to be monitored. Continuous monitoring of the radiation in space is required. Long exposures, on the order of days to years, could accentuate fatiguing of the structure and affect its load carrying capacity. The damage could be in the form of cracks caused by internally induced stresses. The significance of cracks will be discussed in the next paragraph. The effects of radiation on vehicle systems is discussed in detail in Volume II of this study.

Perhaps the greatest single event which could cause the failure of a vehicle is the impact and penetration by a hyper-velocity solid particle. If the penetration is large enough, rapid decompression will occur. Smaller penetrations will cause pressure leaks, the rate of which is a function of hole size and internal-external pressure ratio. Smaller particles of lesser energy will impinge upon the vehicle causing surface erosion. Abrasive action of such particles can, over a period of time, alter the radiative properties of the vehicle skin. The sputtering by impact with high velocity atoms and molecules will also contribute to this effect. The cumulative effect of surface erosion, solar radiation, and sputtering could lead to large thermal gradients which could be hazardous to the internal components of the vehicle. Also, the effect of radiation and meteoritic impingement hurries the onset of cracks leading to structural failure and leaks.

Another environmental condition which affects the vehicle is the presence of continuous high vacuum. While the high vacuum may affect the material properties and perhaps hasten the evaporation or sublimation of certain alloying elements of materials or could lead to increased friction and tend to dry weld bearing surfaces, the main source of hazard stems from the requirement to insure a habitable atmosphere for manned flight. Any leak caused by combined spatial environments can be aggravated by the pressure differential across the vehicle pressure shell. This pressure differential requires continuous monitoring in order to assess leak rate hazards.

The above analysis indicates that the following parameters should be monitored to insure vehicle safety:

(1) Aerodynamic temperature rates

(2) Pressure - dynamic and ambient

(3) Structural strain

(4) Structural vibration and acceleration

(5) Radiation dose rates and integrated doses

(6) Micro-meteorite erosion rates and/or momentum and flux rates

(7) Acoustic noise

The present state of the art of instrumentation to monitor the above parameters is presented in the following section.

## SECTION II

## INSTRUMENTATION STATE OF THE ART

### A. Temperature Measurement

It has been established that temperature is one of the most significant environments. This is particularly true during re-entry where elaborate measures in both material selection and construction have to be taken to assure the survival of the vehicle.

Figure 1 shows normal temperature ranges of transducers which will provide proportional signals to remote instrumentation. The transducers most commonly used are:

(1) Radiation pyrometers

(2) Thermocouples

(3) Resistance thermometers

(4) Filled thermometers

(5) Thermal sensitive coatings

Radiation pyrometers require major development for airborne use. They are used primarily for ground installation.

Filled thermometers are not applicable for surface measurements. Thermal sensitive coatings are attractive for surface measurements, but at present do not have the required temperature range.

The transducers found most applicable for the measurement of vehicle surface temperatures are thermocouples and resistance thermometers. This discussion of the state of the art will be limited to them.

#### 1. Resistance Thermometers

A point of departure for the investigation of suitable heat flux measuring devices is the instrumentation used in the simulation of hypersonic re-entry conditions in shock tubes. These instruments are characterized by fast response to the transient flow of the shock tube.

In other respects, too, such as range, sensitivity, and ruggedness they would meet the requirement of space flight. One such instrument is a resistance thermometer with a rise time of less than a microsecond consisting of a thin metallic film (a few microns thick) mounted on glass for the measurement of transient surface temperatures on models in a hypersonic shock tunnel (Ref. 46). Furthermore, by mounting the film on an insulator such as glass instead of metal, high sensitivity to heat transfer at a sacrifice of rise time is achieved. Conventional heat transfer instruments consist of two temperature sensors separated by an insulator with known thermal properties. By measuring the two temperatures, the heat transfer rate can be calculated using Newton's Law of cooling. This method is not practical for transient measurements since the heat has to penetrate a finite distance into the material.

A more direct method of measurement is to make the instrument of homogeneous material and to measure the surface temperature of the material. The film resistance change is a function of surface temperature and is related to the heat transfer rate.

These relations based on heat transfer theory are:

$$q = 1/2\sqrt{\pi K\rho C_p}\left(\frac{T(t)}{\sqrt{t}}\right) \quad \text{, for constant heat rate} \qquad (1)$$

$$q(t) = \frac{1}{\pi}\sqrt{\pi K\rho C_p}\left(\frac{d}{dt}\int_0^t \frac{T(\lambda)\,d\lambda}{t-\lambda}\right), \quad \text{for varying heat rate.} \qquad (2)$$

where

$q$ = heat transfer rate

$T$ = surface temperature

$t$ = time

$K\rho C_p$ = properties of the material conductivity, density, and heat capacity

$\lambda$ = a computational quantity

As these expressions show, the transient surface temperature is related to heat transfer rate and the properties of the material. The miniature thin-film resistance thermometer gages have been used at Cornell Aeronautical Laboratory to determine experimentally heat transfer rates in shock tubes. These results correlate well with theoretical predictions.

Similar instruments are used to measure temperature fluctuations in the inlet of jet aircraft. They have the following characteristics.

Instrument diameter - 1/5 inch.

range from -65 to 1000°F

accuracy - $\pm 2^{\circ}$F throughout range.

The upper limit of temperature could be extended by choice of better bonding material of metal film to glass. This instrument could be adopted to measuring transient radiation heat transfer. A possible technique would be to mount the thermometer between two layers of glass to prevent other modes of heat transfer. As a further refinement, the spectral distribution of the radiant heat can be analyzed by selecting various type glasses with selective passbands.

2. Thermocouples

There are numerous thermocouples available for different high temperature ranges. Copper-Constantan couples are usable up to 500°F. Iron-Constantan couples are applicable to 1500°F. Chromel-Alumel couples are used to 2300°F. Platinum-vs-platinum plus rhodium couples are usable to 3000°F, and super-temperature couples used to 4000°F are under development.

A complete study of the state-of-the-art of temperature transducers has been carried out by Knorr of Bell Aircraft (Ref. 11) and by Lampert, et al of Aeronautronic Division of Ford (Ref. 48). Another description of these devices at this time would be repetitive and therefore will not be presented; the reader is referred to the two references mentioned above. Table 1 and Figure 2 will serve as a guide in the selection of proper thermocouples.

For the measurement of heat flux from the external to internal surfaces of a hyper-velocity vehicle, thermocouples can be placed on parallel surfaces and $\frac{dT}{dt}$ can be determined (T=temp, t = thickness). (The thermal flux over a surface can be determined by strategically locating the sensors in a set pattern in the direction of flow.)

The biggest problem in the application of thermocouples to surface measurements is the method of contact. The presence of the thermocouple in a fluid flow gives rise to mass and surface discontinuities occasioned by the sensing element which upset the convective flow, and transfer heat away from or into the contact area at a greater rate than may be experienced in cases where the discontinuity does not exist.

TABLE 1

THERMOCOUPLE CHARACTERISTICS

| Type | Composition | Temp. Range °F | Max. Temp. °F | Melting Temp. °F * | Polarity | Limit of Error |
|---|---|---|---|---|---|---|
| Platinum and Rhodium Platinum | 100% 10% 90% | 0 to +2650 | 3100 | 3220 3320 | - + | ±0.5% |
| Platinum and Rhodium Platinum | 100% 13% 87% | 0 to +2650 | 3100 | | - + | ±0.5% |
| Chromel-Alumel | 90% Ni 95% Ni 10% Cr 2% Al 2% Mn 1% Si | 0 to +2200 | 2450 | Approx. 2600 | + - | ±0.75% |
| Iron-Constantan | 99.9% Fe 55% Cu 45% Ni | -300 to +1400 | 1800 | 2790 2170 | + - | ±0.4% |
| Copper-Constantan | 99.9% Cu 55% Cu | -300 to +700 | 1100 | 1980 2170 | + - | ±0.4% |
| Tungsten-Iridium | 100% W 100% Ir | 1800 to 3600 | 4000 | 4500 | | ± .5% |

* In order of listing under type

If the sensing element is brought into the flow from the unheated side of the surface material, the temperature gradient along the sensing element lead wires is excessive. If the rate of surface temperature rise is several hundred degrees per second, this temperature gradient results in faster cooling than would be experienced under lower rise rates. Disturbance of the surface heat sink material can change the heat conductive properties at the point of contact (Ref. 59).

The most logical solution is to arrange the temperature sensing device in an isothermal field on the exposed surface. It is then necessary to insure that the sensing element is not exposed directly to thermal flux unless it is an integral part of the surface and has the same thermal characteristics as the surface material. This seems to be beyond the present state of the art and requires further development. There are ceramic insulators and ceramic cements which have properties close enough to that of the surface material which can be used to attach the device to the surface. It is necessary to peen or mount the device flush with the surface in order not to disturb the fluid flow.

3. Others

Table 2 is a summary of commercially available temperature-measuring instruments or systems (Ref. 76).

## B. Pressure Measurement

When considering the safety of a high-altitude vehicle operating in the vacuum of space and the dense atmosphere during high-speed re-entry, the following pressure instrumentation is necessary.

The internal pressure of the vehicle must be maintained at safe levels for both the pilot and the equipment. However, events may occur which will alter the internal pressure. Particle puncture in space will cause a pressure leak, the rate of which is a function of puncture hole size and the internal-external pressure ratio. In this instance it is absolutely imperative that the leak rate of cabin air be monitored continuously for pilot and equipment safety. This will require internal pressure gages or leak-rate gages.

As the vehicle descends at hypersonic velocity into the dense atmosphere of the earth or another planet, forces build up on the external structures which are a function of the air density and speed of the vehicle. These forces are due to the dynamic pressure which any high-speed vehicle will experience. If these loads are excessive as a result of too fast a descent into the atmosphere, the structural integrity of the vehicle may be jeopardized. It is therefore essential to continuously monitor the dynamic pressure distribution over the critical surfaces of the vehicle.

TABLE 2.

SUMMARY OF INFORMATION REGARDING COMMERCIALLY AVAILABLE TEMPERATURE-MEASURING INSTRUMENTS OR SYSTEMS

| Kind of instrument | GLASS STEM (LIQUID-IN GLASS) | | BIMETAL | FILLED SYSTEMS | | | THERMOCOUPLES | | | | RESISTANCE THERMOMETERS | | | | RADIATION PYROMETER | OPTICAL PYROMETER | PYROMETRIC CONES | MELTING PELLETS |
|---|---|---|---|---|---|---|---|---|---|---|---|---|---|---|---|---|---|---|
| | Mercury | Other Liquids | | Vapor Pressure | Liquid-Filled | Gas Filled | Iron/Constantan | Chromel/Alumel | Copper/Constantan | Platinum/Platinum-Rhodium | Platinum | Copper | Nickel | Thermistors | | | | |
| Low temp limit | -38°F (-39°C) | -321°F (-196°C) (pentane) | -100°F (-73°C) | -427°F (20°K) | -125°F (-87°C) | -452°F (4°K) | about -320°F (-196°C) | about -300°F (-184°C) | -424°F (20°K) | commonly 32°F (0°C) | -300°F (-184°C) | -220°F (-140°C) | -300°F (-184°C) | -76°F (-60°C) (most types) | about room temperature | 1400°F (760°C) (normally) | 1085°F (585°C) | 113°F (45°C) |
| High temp limit | 1100°F (593°C) | | 1000°F (538°C) | 600°F (316°C) | 1200°F (649°C) | 1000°F (538°C) | 1400°F (760°C) in oxidizing atm 1800°F (982°C) in reducing atm 2000°F (1093°C) spot readings | 2100° to 2300°F (1149° to 1260°C) 2400°F (1316°C) spot readings (not to be used in reducing atm) | 660°F (349°C) 930°F (499°C) spot readings | 2600° to 2800°F (1427° to 1538°C) 3216°F (1769°C) spot readings. (not to be used in reducing atm) | 1400° to 1800°F (760° to 982°C) | 250°F (121°C) | 600°F (316°C) | 750°F (399°C) (glass coated) | as high as desired | as high as desired | 3659°F (2015°C) | 2588°F (1371°C) |
| Remarks | Low price. Reasonable accuracy. Easily broken short scale length | | Easier to read than liquid-in-glass. Sometimes damaged by overheating | Normally has nonlinear scale. Has cross-ambient effect. Cheapest of the filled systems | Can be compensated accurately for ambient temperature variations | Suitable for wide ranges. Linear scale. Requires large bulb | Thermoelectric Power, Microvolts per Degree C | | | | (R 100°C - R 0°C)/100 R 0°C | | | | Can operate a recorder and automatic controls. | Cannot operate a recorder or automatic controls. | Indication somewhat affected by heating rate. | |
| | No auxiliary equipment required | | | | | | 64 at 760°C | 38 at 1100°C | 41 at 25°C | 12 at 1200°C (alloy 10% Rh) 14 at 1200°C (alloy 13% Rh) | 0.0039 | 0.0043 | 0.0066 | -0.0098 (one type) | | | | |
| | | | | | | | The couple most widely used in industry. Poor reproducibility above 1600°F (871°C) | Chromel is 90 Ni, 10 Cr (chromel P). Alumel is 94 Ni, 3 Mn, 2 Al 1 Si. | Constantan is 57 Cu, 43 Ni | Expensive | May drift at the higher temperatures. | | | High sensitivity. Only fair stability. | Absorbers of radiation, such as windows or dirt, can affect accuracy. Emissivity of source important. Very rapid response. | | A single cone or pellet can indicate only its rated temperature, and is normally used only once. | |
| | Can give very rapid response, matched only by the radiation and optical pyrometers. | | | | | | | | | | Give greater accuracy than thermocouples, for the same investment. High sensitivity makes them suitable for narrow-range instruments. | | | | | | | |

1. Leak-Rate and Internal Pressure Transducers

Internal cabin environmental pressure conditions can be determined continuously by either measuring the change in pressure of the cabin air or the leak rate of cabin air. The effectiveness of measuring pressure changes within the cabin is limited by the fact that to detect any pressure change in a large cabin, a large loss of air will be required. Thus, there may be an appreciable loss of air before any pressure drop is detected. This problem requires pressure gages of high sensitivity.

However, it may be more practicable to monitor the leakage of the cabin air continuously. Leak-rates will be more easily detected than will a slight change in pressure. But, leak rates from fatigue cracks and minute meteoroid penetrations will be quite small and exceedingly difficult to detect and locate from the inside of the cabin during flight. Leakage of this nature would be significant primarily because of this loss of gas which must necessarily be replenished from reserve supplies of oxygen and nitrogen.

Internal pressures will vary from sea level, 760 mm (14.7 psia) which is ideal, to 30,000 ft, 280 mm Hg, (4.36 psia) which is the critical altitude for decompression sickness. To avoid hypoxia, the partial pressure of oxygen should not fall below 110 mm Hg and should preferably be at 160 to 180 mm Hg.

The range which the instruments must monitor is from sea level (760 mm Hg) to 110 mm Hg. The main factors which determine the instrument requirements are sensitivity and speed of response. The following example will illustrate the problem of determining sensitivity and response time.

Meteorite penetrations of a sealed space cabin probably offer the greatest hazard to manned space flight. Whipple (Ref. 45) has calculated the probability of penetration by meteoroids of various sizes. Konecci (Ref. 44) has derived the basic equations for satellite decompression. The problem which concerns us is the detection of a leak within the cabin and the measurement of leak-rate and/or pressure drop. To attack the problem in a practical way, certain assumptions can be made of a hypothetical space mission. A mission of one year's duration is assumed in which the cabin of 500 cubic feet volume is pressurized to 14.7 psi; the cabin skin thickness is 0.125 inch.

According to Whipple, the largest meteoroid to expect during a one-year mission is 0.129 diameter (the probability of penetration is one in 234 days). For decompression limits 4.36 psi is selected as the lower pressure limit. It is at this pressure that decompression sickness occurs. Based on flow equations, Konecci derived the equation for the escape of air from a satellite.

$$dW/dt = -K\ W\ A\ C/V\ 144\ pps \tag{3}$$

where W = instantaneous weight of the enclosed air (lbs).

K = orifice coefficient which is assumed to be 1.

A = orifice area in square inches.

C = speed of the escape air, which equals the speed of sound.

V = volume of the enclosed air in cubic feet.

Separating the variables,

$$dW/W = -ACdt/144\ V \tag{4}$$

Assuming an isothermal change, the thermodynamic equation of state gives:

$$dP_c/P_c = dW/W \tag{5}$$

where $P_c$ is the instantaneous cabin pressure.

Equation (4) can be written as:

$$dP_c/P_c = -ACdt/144V \tag{6}$$

Integrating Equation (6),

$$t = (144V/AC)\ \ln\left(\frac{P_{co}}{P_c}\right) \tag{7}$$

These derivations are based on two assumptions.

(1) The cabin exhausts to an infinite volume, or a vacuum.

(2) The flow through the orifice is sonic. Therefore, the outside pressure ($P_a$) must be low enough that the ratio $P_c/P_a$ exceeds the critical pressure, or $\left[2/(n+1)\right]^{n/n-1}$, where n is the exponent which varies from 1 for isothermal expansion to 1.4 for adiabatic expansion. The decompression time from 14.7 psi to 4.36 psi can be calculated. From Equation (7),

$$t = (144V/AC) \ln\left(\frac{P_{co}}{P_c}\right)$$

in the hypothetical case,

$$V = 500 \text{ cu. ft; } A = \frac{\pi(.129)^2}{4} \text{ sq in, } C = 1130 \text{ fps}$$

$$P_{co} = 14.7 \text{ psi and } P_c = 4.36 \text{ psi}$$

substituting,

$$t = \frac{144 \times 500}{\frac{\pi(.129)^2 \times 1130}{4}} \ln\left(\frac{14.7}{4.36}\right)$$

solving,

$$t = 5950 \text{ secs.}$$

This indicates that emergency procedures and repairs must be initiated and completed in less than 5950 sec (1.65 hours).

In order to select an instrument to detect a tolerable pressure drop and determine the required response time of the instrument, a pressure drop of 0.10 psi is selected as a tolerable drop. Using equation (7) and solving for t, t = 34.2 sec.

In effect, this indicates that a suitable pressure gage should have a response time of less than 34 secs. However, allowing for errors in the assumptions and the fact the C changes as a function of pressure and temperature, a safety factor of 2 is incorporated. This means that the pressure gage has a response time of 17 secs. Many commercial instruments are available to satisfy this requirement. Sensitivity of 0.10 psi full scale (15 psi to less than 4.36 psi) may be more difficult.

The following gages and their pressure ranges are currently available:

(1) Precision dial-type instruments.

(2) Stacked diaphragm gages.

(3) Pirani gages (thermal) 100 mm Hg to $10^{-3}$ Hg.

(4) Ionization gages 0.50 mm Hg to $10^{-8}$ mm Hg.

(5) Aneroids - referenced to outside vacuum.

(6) Haven's cycle gage 760 mm Hg to $10^{-5}$ mm Hg.

The conventional pressure gages listed below have been described in detail in the literature (Refs. 9, 10, 11, 12, 13, 14, 15, 18) and will therefore not be repeated here. However, those instruments which play a direct role in the monitoring system are presented here. The descriptions include special features which qualify the instrument to measure internal pressure changes. Figure 3 shows the useful pressure ranges of vacuum measuring instrumentation.

Standard instruments are used to cover the pressure range from atmospheric to 1 mm Hg absolute. These units are comparable to the precision dial type indicators, which cover essentially the same range. Precision dial type instruments are generally available in two types, one of which has an accuracy of 1 part in 300, another longer scale unit having an accuracy of 1 part in 1000.

All of these instruments have reasonably good repeatability and can measure pressures effectively down to about 2 mm without introducing serious errors. All of them have the disadvantage that they are direct indicating devices and should be, for accurate readings, close coupled to the vacuum system involved.

The pressure range from atmosphere to 1 mm can also be covered by the mechanical type transducer which usually consists of a stacked diaphragm-type movement. The diaphragm moves an electrical element, which can give a remote indication of system pressure. Elements generally consist of a variable resistance winding or parallel plates to provide a variable capacity. In either case, sensitivity of reading is of the order of 1 part in 1500. Readability, however, is determined entirely by the sensitivity of the read-out equipment. Generally speaking, the mechanical transducer element when properly made has good resolution and repeatability and presents very little hysteresis error. It is believed that 2 mm is their effective limit of reading with any degree of accuracy, although some indication can be obtained to approximately 0.5 mm.

Still another system is available for pressure measurement between atmosphere and 1 micron. This consists of the radium activated ionization gage which covers the full scale between 1000 mm and $10^{-3}$ mm. This pressure scale is covered in six ranges, all of which are linear. The instrument is suitable for direct indication or recording and provides a most convenient means of pressure measurement. As the scale ratio used in this instrument is based on powers of 10, the readability becomes greater on the lower scales. The minimum readable increment on the top scale equals 10 mm; on the lowest scale, the minimum readable increment is 0.0001 mm. The instrument therefore provides

its greatest readability in the range from 100 mm to 1 micron. A drawback, however, is the fact that the d-c amplifier utilized in the instrument must be zero balanced after each range change to provide accurate readings. Without this adjustment, serious errors can occur as the zero shift can be considerable, presenting a problem if it is desired to use recording equipment. Instrumentation can be provided, however, which will give automatic correction to this zero shift problem, thereby allowing the use of automatic range changing if desired. This instrument, like thermal conductivity type units, is also affected by the gases present in a system. However, it will give reasonably accurate readings in a system containing essentially air. Over-all equipment accuracy is of the order of 3%.

2. Dynamic Pressure Measurement

A hypersonic vehicle maneuvering within the atmosphere will be subjected to dynamic surface pressures which are a function of the vehicle speed, shape, angle of attack and the atmospheric density. Conventional methods of surface pressure measurement are limited in altitude capability to heights less than approximately 90 to 100 KM, since at this level the mean free path of the gas particles becomes long with respect to sensing device's dimensions.

There are many high pressure transducers available today. However, certain physical characteristics of the boundary layer surrounding the vehicle impose limitations on the gages. To make accurate measurements of the dynamic pressure profile on the surface, it will be necessary to mount the pressure transducers flush with the vehicle surface to avoid disturbance of the flow.

For measuring nose cone pressures during hypersonic re-entry a device called the Q-ball has been designed by the Nortronics Division of Northrop Aircraft Company.

For measuring surface impact pressures, a diaphragm-type pressure transducer has been designed by the Lockheed Aircraft Company. This gage measures the impact pressures external to a re-entering vehicle without ports through the vehicle shell. Each of the above devices are considered a major advance in the state of the art of dynamic pressure measurements. Details of other dynamic pressure gages may be found in the literature (Ref. 11, 18, 19, 22, 24, 25) and will not be discussed here. For purposes of presenting the latest in the state of the art, the Q-ball and diaphragm transducer gages are discussed next.

a. Q-ball

The Q-ball, designed for use on the X-15 re-entry vehicle, measures angle of attack, sideslip angle, and dynamic pressure during re-entry. Figure 4 shows a functional diagram of the device. Pitot pressure is picked up on the

differential pressure transducer. The 400-cps output signal of the transducer is amplified in both the preamp and the gain changing amplifier. Changes in dynamic pressure of 15-2500 psf are measured. This change in dynamic pressure is transferred to a resistance change within the circuit. The sphere's orifice layout is designed to give dynamic pressure information over a wide range of Mach numbers. A control and a displaced orifice sense the sphere pressure gradient.

The performance of the Q-ball sensor is tabulated below.

Positional Accuracy - $\pm$ 0.25 deg (nominal).

System Threshold - 0.001 psi (max).

Frequency Response - 3 db at 7 cps.

Velocity - 240 deg/sec.

Velocity Error - 1 deg at 60 deg/sec.

Q-compensation - Gain-compensated for dynamic pressure range of 15-2500 psf.

Stagnation Temperature - 4000$^{o}$F (max).

Altitude - Sea level to 300,000 ft.

Mach Number - 1-10.

Gimbaling and conventional actuator linkages, with their usual friction problems, are avoided by using rotary actuators that are coaxial with the sphere's axes of rotation. Direct coupling to the sphere completely eliminates backlash.

b. Diaphragm Pressure Transducer

In a closed pressurized vehicle it may not be permissible to use pressure ports on the surface. This restriction eliminates a great many commercial pressure transducers for consideration. Commercial flush cell diaphragms are very thin and extreme care to avoid over-pressure must be taken. Again commercial transducers are not satisfactory for this purpose.

On re-entry vehicles, neither of the above methods can be used because of the aerothermodynamically-smooth, mechanically-rigid surface required and because of the high input heat rates over the surface during re-entry. Wrathall of Lockheed (Ref. 21) has devised a diaphragm type pressure transducer

where the diaphragm of the gage is made an integral part of the surface coating. If a surface hole is located at the point where the pressure is to be measured and if, before surface coating, a tailored plug is inserted in the hole and coated simultaneously with the rest of the surface, except for a thin annular ring around the outside edge of the plug end, a rigid-center fixed-edge diaphragm is produced (Figure 5). The plug must be in good thermal contact with the diaphragm; this is done by plating the diaphragm on the plug. Any resulting deformation is distributed over the total plug area, which is helpful in preventing flow separation. Any applied force will deflect the diaphragm and stress the measuring transducer.

c. Magnetostrictive Pressure Transducer

Wrathall also has developed variations of the above method which differ only in the measuring transducer. Figure 6 shows a magnetostrictive device. The device shown was not justified for surface pressure applications because of the large deflections involved (Ref. 21). However, under certain conditions this device is rigid enough and can be produced mechanically rugged with desirable electrical characteristics. Magnetostrictive materials are temperature sensitive and therefore temperature compensation is imperative.

d. Strain-Gage Pressure Transducer

There are two types of strain-gage transducers, the unbonded and the bonded. The bonded gage shows better temperature compensation but the unbonded-strain-gage transducer is very sensitive to temperature effects and, in particular, to temperature gradient (Ref. 22). This type of gage has a simple diaphragm as the structural member and a strain gage mounted behind the diaphragm to detect the deflection due to the applied pressure. A temperature compensating arrangement used in unbonded-type transducers make them better suited for high-temperature application than the bonded type.

A strain-gage sensing-element with a set of four active arms arranged in a Wheatstone bridge is a well-known compensating configuration. This arrangement gives effective transient-error compensation if the temperature gradient between each of the four arms and the heat source remained the same during the temperature transient period. Figure 7 shows a compensated and standardized unbonded strain-gage pressure transducer. This type of gage can be used in pressure ranges from 10 psi to 7000 psi at temperatures to 300°F.

For higher-temperatures and flush-mounted operation, a water-cooled diaphragm must be used. The basic principle is to design a diaphragm with ample cooling, high strength; and high flexibility.

A catenary type diaphragm gage can be used at temperatures as high as 3000°F for a few minutes and 1000°F for sustained periods. A catenary type diaphragm

gives a more accurate pressure distribution than the conventional flat diaphragms. The motion of the diaphragm moves two arms of a Wheatstone bridge that are wound perpendicular and parallel to the movement of the diaphragm.

A unique method for providing even diaphragm cooling has been developed by Dr. Li (Ref. 22). Figure 8 shows the unique configuration. In this arrangement a double spiral cooling passage cools the diaphragm evenly and elininates any hot spots. There are two diaphragms involved. The outer diaphragm, facing the fluid flow, is supported by the double spiral ribbon, which is, in turn, supported by the inner diaphragm. This inner diaphragm has a rigid center-disk and a thin V-groove to receive the wider portion of the spiral ribbon.

A water jacket exists between the two layers of the shell structure. The outer diaphragm covers both layers so that any thermal stress generated in the outer shell will not be transmitted to the inner shell. A gage of this type with water jacket and double spiral diaphragm has been used in rocket tests and has withstood temperatures up to 5000°F (Ref. 19). Even without water cooling and using a compensating arrangement this gage is very stable at high temperatures.

For complete details on these type of pressure transducers the reader is referred to Reference 19 and 22 which cover some of the most recent advances in dynamic pressure measurement techniques.

C. Strain Measurement

Strain has been established as one of the structural parameters to be continuously monitored for vehicle safety. Strain is one of the most basic measurement values in the analysis of a structure. Currently, strain measurements are made with bonded, variable-resistance wire gages and their room-temperature properties are well known.

However, at the increasingly high-flight temperatures that a hyper-velocity vehicle encounters, changes occur in strain gage behavior that pose difficult new problems. The most important of these changes are (Ref. 61):

(1) The electric resistance of the gage wire changes.

(2) The wire, the structure, and the bonding cement undergo thermal expansion.

(3) The electric insulating value of the cement changes.

(4) The strain sensitivity of the wire changes.

(5) The gage and the structure oxidize and corrode more readily.

(6) The organic cements begin to lose their strength and decompose.

Among the suitable gage materials are the copper-nickel (Advance), nickel-chromium (Nichrome V), and nickel-chromium-aluminum (Karma) alloys. Another class of materials that is under development as strain-sensitive elements is the iron-chromium-aluminum series. Among these, alloy D has received the greatest attention. (Ref. 60).

For temperatures below 550°F, the copper-nickel alloys are most commonly used because of superior cost, stability, gage factor, and resistivity characteristics. Above 550°F, this material suffers from intergranular corrosion. Karma is competitive with Advance below 550°F, and greatly superior in the temperature range up to 800°F. Above 800°F, Karma undergoes a metallurgical transformation and becomes unsuitable.

Nichrome V is metallurgically stable up to 1000°F. It has been used as high as 1200°F, but its high-temperature coefficient of resistance makes it very sensitive to small inaccuracies in temperature determination.

Armour alloy D has been tested for strain measurements to 1600°F. Although it does not undergo phase changes, it has a large apparent temperature coefficient of resistivity when mounted as a strain gage.

Strain gage transducers are classified into two categories: bonded and unbonded. In the bonded type, a grid or helix of fine strain gage wires is bonded to a member which is subject to strain upon application of the force being measured. In the unbonded type, a specially designed structure is used to impose a strain on the wires proportional to the load. The strain wires are usually arranged in the form of a Wheatstone bridge. The active elements are arranged so that opposite legs of the bridge increase (or decrease) their resistance at the same rate for a given direction of displacement.

Bonded strain gages have the following advantages:

(1) Excellent linearity and hysteresis may be obtained.

(2) Low sensitivity to temperature effects.

(3) Low sensitivity to shock and vibration.

(4) May be excited by a-c or d-c.

(5) Continuous resolution.

(6) Static or dynamic response.

Some of the disadvantages are:

(1) Low sensitivity.

(2) Limited temperature range.

(3) Lower range limitations.

In the unbonded strain gage, a group of fine strain-sensitive filaments are wired between a fixed frame and the force-summing member. The filaments are arranged in the form of a Wheatstone bridge. When the force-summing member is displaced, the bridge is unbalanced to produce an electrical output which is directly proportional to the applied force.

The advantages of unbonded gages are:

(1) Excellent frequency response.

(2) Low sensitivity to vibration and shock.

(3) May be used to measure static or dynamic phenomena.

(4) May be excited by a-c or d-c.

(5) Small volumetric displacement.

(6) Continuous resolution.

(7) Requires simple resistive balance.

(8) Not effected by electromagnetic fields.

(9) Temperature effects can be easily compensated.

Some of the disadvantages are:

(1) Low output.

(2) Manufacturing complexity.

For use in space vehicles, strain gages should have the following characteristics (Ref. 48):

Operating upper temperature limit: 2000°F.

Strain Ranges: 0-1000 to 0-20000 microinches per inch.

Resolution: 5 microinches per inch.

Accuracy: 1% of full scale output.

In addition the gage should be:

(1) Easily cementable or weldable to any desired surface. Low temperature curing is preferable, but not essential.

(2) Insensitive to, or compensated for, pressure fluctuations, salt, or acid corrosion, magnetic and electric fields, humidity, and acceleration.

(3) Able to survive repeated temperature cycling without deterioration in performance.

There is no gage presently available which will satisfactorily fulfill all of these requirements.

D. Vibration and Acceleration Measurements

It has been established that vibration caused either mechanically and acoustically by the rocket engines, or aerodynamically by the boundary layer surrounding the vehicle has a deleterious effect on the vehicle and its structure. The most critical periods of vibration occur during the boost and re-entry phases of the vehicle trajectory. Vibration is to be monitored during these phases for vehicle safety and reliability.

Many types of vibration transducers are available. Systems have been designed to measure directly either displacement, velocity, or acceleration, and to differentiate or integrate the result to obtain the other two quantities.

The most practical parameter to measure for vibration is usually acceleration (Ref. 69). The more common type vibration transducers are the ceramic crystal accelerometer, strain-gage accelerometer, strain-gage angular accelerometer, and the rotating pendulum accelerometer.

The accelerometer employs an elastically suspended mass as part of its sensing system. The mass is mounted on springs, and the system (springs and mass) has a high natural frequency. This natural frequency must be well above the frequency of the vibrating object. A sensing element within the pickup detects the force exerted on the suspended mass and converts it into an electrical signal. Since transmissibility between the suspended mass and case is, for practical purposes, one, and force is proportional to acceleration, the electrical signal (when properly calibrated) is a measure of case (and vibrating object) acceleration.

1. Crystal Accelerometers

Piezoelectric crystals generate electric charges on their surfaces when placed under stress. In the crystal accelerometer one or more crystals are mounted so that acceleration forces produce the stress. The quantity of the charge induced is proportional to the applied stress, which, in turn, is proportional to the acceleration.

There are two types of crystal accelerometers, the compression and the bimorph (bender) types (Ref. 72). Figure 9 shows the cross-section of the compression-type crystal accelerometer. This type consists essentially of a cylindrical assembly in which a mass, under acceleration, compresses one or more disc-shaped crystals. The crystal faces are coated with a conducting material and are connected either in series or parallel. These accelerometers generally have relatively high impedances, high natural frequencies, and high ranges, and can be designed for high-temperature operation.

The bimorph-type accelerometer shown in Figure 10 contains two thin crystal slabs each fastened to either side of a metallic shim. Both sides of both crystals are coated with a conducting material. The crystals are oriented so as to be connected in series or parallel. The crystal slabs may be center-supported or end-supported. This type has a smaller "g" range than the compression type.

There are many types of crystals, the most important being quartz, Rochelle salt, ammonium dihydrogen phosphate (ADP), and barium titanate. Barium titanate is the most versatile, being artifically produced in any size and shape for differenent pickup designs. It has good high-frequency response and is less subject to changes in sensitivity due to aging. It is less temperature sensitive than the others. Starting at 80°F, the output typically drops only 0.1 percent for each degree of temperature change, either increasing or decreasing. For temperatures encountered by a vehicle during boost and re-entry, the output drop could be substantial unless adequate thermal protection of the accelerometer is provided.

2. Strain-Gage Accelerometers

Strain-gage accelerometers use resistance-wire strain gages as the sensing elements. A mass, suspended by either the resistance-wire gages directly or by cantilevers to which the resistance-wire gages are cemented, provides the force which changes the wire resistance. The resistance change is usually measured by a Wheatstone bridge circuit. **Natural** frequencies range from 40 cps to 200 cps. This type of accelerometer is also subject to static accelerations, and in choosing the proper instrument, the required range is determined by the sum of the static and dynamic accelerations.

Wire strain gages are temperature sensitive and must be thermally shielded to yield accurate results.

3. Strain-Gage Angular Accelerometers

Unlike the previous accelerometers which have been linear accelerometers, this type uses the strain-gage principle to measure the angular acceleration on a rotating or revolving body. These devices can be used to measure roll, pitch, and yaw angular accelerations. These accelerometers are used in the very low frequency range of 0 to 20 cps.

4. Rotating Pendulum Accelerometers

This device is unique in that it measures with extreme accuracy, very low levels of acceleration on the order of $10^{-4}$ to $10^{-10}$ g (Ref. 70). This type of accelerometer may find use in low-thrust space vehicles which use solar radiation pressure as the propulsion source. The accelerations encountered by this type of vehicle, the photon rocket and the ion rocket, are of the same magnitude of those above. A complete treatise on the pendulum accelerometer may be found in Reference 70. A possible rotating pendulum accelerometer configuration is shown in Figure 11.

The pendulum mass is in the form of an unbalanced cylinder. To overcome losses due to drag and friction in the bearing, a driving torque in the form of an air jet is provided to sustain the rotation of the unbalanced mass. The quantity measured with this device is time ($\Delta t$). The period of mass rotation is a function of the applied acceleration. Neglecting damping, the equation of motion is

$$I \frac{d^2 \theta}{dt^2} + mar\sin\theta = 0$$

where

$I$ = moment of inertia

$m$ = mass of pendulum

$a$ = acceleration of center of suspension

$r$ = displacement of center of gravity (CG) from center of displacement

$t$ = time

$\frac{d^2 \theta}{dt}$ = angular acceleration

$\theta$ = angular displacement

E. Radiation Measurement

The radiation of concern is that found in the inner Van Allen belt emanating from the sun and trapped in the earth's magnetic field. This radiation consists of protons and electrons, which have sufficient energy to penetrate the shell of a space vehicle at altitudes above 1000 KM. The problem arising here is the formation of secondary particles caused by a primary colliding with the vehicle. By far the most energetic particles to contend with re the high energy protons known to exist in an area of $40^{\circ}$ of latitude centered about 1900 KM above the geomagnetic equator. These particles have been found to have energies between 75 mev and 700 mev with an average at about 100 mev. It is these "hard" particles which will penetrate a vehicle shell.

The radiation dosages found in space varies from 10 to 100 roentgens per hour depending upon whether electrons or protons are considered. However, during increased solar flares, radiation levels exceeding 500 to 1000 roentgens per hour are to be anticipated.

Since the launching of the first earth satellites, numerous radiation detection experiments have been carried out. Innumerable radiation instruments have been employed. These consist of geiger tubes, scintillation counters, Cerenkov counters, ionization chambers, photographic emulsions, and many others. Numerous radiation detectors are currently available for use in high-altitude vehicles for monitoring both external and internal environments.

1. External Radiation Detectors

Ionization chambers (Ref. 18, 27, 28, 29, 31, 32, 38, 41) measure the ionization produced within a gas-filled chamber by a flux of radiation. They do not measure the number, energy, or composition of the radiation directly but sometimes can furnish some of this information by other means. Ionization chambers can be made quite reliable, have extremely long useful lifetimes and can be designed for almost any kind of radiation environment.

Besides responding to primary radiation, the chamber will respond to secondary particles resulting from the interaction of the primary particles with the chamber walls and with the material surrounding the chamber. This could lead to increased ionization within the chamber. Thus, the ionization chamber can at most yield a qualitative idea of the nature of the radiation present. Therefore, the ion chamber yields a direct measure of the number of roentgens equivalent man (REM) in the region where the chamber is located. This device is applicable for radiation dose measurements both internal and external to the vehicle.

2. Scintillation Counter

A scintillation counter is used to measure the energy of a particle incident on a scintillating coating. When an energetic charged particle penetrates the coating, the coating emits a flash of light. The light, trapped by a reflector, is converted into a pulse of current by a photomultiplier tube. The minimum energy detectable is determined by the coating thickness. This device can be used for measuring the energy of the incident primary particles external to the vehicle. Typical scintillators are described in detail in the literature (Ref. 36, 27) and are reviewed here briefly.

a. Electron Detector

Dr. L. Davis of NASA has proposed a scintillation type electron detector for use in a space probe. A schematic drawing of the electron detector is shown in Figure 12. The detector consists of an aperture to define the beam of electrons, a gold scatter disc which fills the solid angle defined by the aperture, and a powder phosphor mounted on the face of a photomultiplier positioned so that the phosphor will intercept a large fraction of any radiation reflected from the gold disc. The multiplier output is a linear function of the incident energy flux for electrons of energy between 10 kev and 200 kev.

b. Ion Detector

A schematic of the ion detector is shown in Figure 13. The detector is a pulse scintillation device. Ions pass through the aperture, strike a thin aluminized powder phosphor, and produce light pulses in the phosphor, the brightness of which are proportional to the ion energy loss in the phosphor. The photomultiplier converts the light pulses to electrical pulses which are then amplified. One rate circuit is set to trigger on pulses corresponding to energy losses greater than 100 kev and a second rate circuit to pulses greater than 1 mev.

The ion detector is insensitive to electrons and x-rays because of the thinness and the particular characteristics of the phosphor used. The decay time of light pulses produced in this phosphor is not constant but is inversely proportional to the square of the energy loss density or ionization density in the phosphor.

c. Total Energy Flux Detector

The geometry of the total flux detector is identical to that of the ion detector. An aperture defines a beam of radiation which directly illuminates an aluminum coated phosphor mounted on a photomultiplier tube. The d-c output of the tube is then proportional to the total energy flux of x-rays, electrons, and ions which can penetrate 0.00005 cm of aluminum and are absorbed in 0.005 cm of aluminum.

d. Electron and Proton Detector

Space Technology Laboratories have designed a scintillation counter to measure the total flux of electrons of energy greater than 225 kev and protons of energy greater than 2 mev. This device is similar to the one proposed by Dr. Davis. The only difference is the thickness of phosphor coating which determines the minimum penetration energy.

e. Geiger-Mueller Tube

A Geiger counter is an ionization chamber in which the applied voltage is high enough for the gas multiplication of the initial ions to produce a discharge that spreads along the length of the center electrode. This discharge quenches itself when the positive ions around the anode lower the field below the multiplication threshold. Such a counter can produce a count when a single electron is produced in the active volume. An excellent description of Geiger counters may be found in the literature (Ref. 43). Figure 14 shows the cross-section of a typical Geiger-Mueller tube.

f. Proportional Counter

A proportional counter is an ionization chamber in which the initial ions are multiplied by collision in a region of high electric field. Such counters are applicable when the initial ionization is lower than that which can be measured using an ionization counter, or where it is desirable for simplicity to eliminate all or part of the amplifier circuit.

g. Proportional Counter Telescope

A proportional counter telescope is used to detect particles more penetrating than those measured by scintillation detectors. A cross sectional view of a proportional counter telescope is shown in Figure 15. Two counters are formed by dividing a tube (1 inch I.D.) in half with a stainless steel partition. Except for an entrance aperture, the counters are shielded by a 10 $g/cm^2$ thick lead cylinder. Particles entering through the aperture will pass through both counters if they have sufficient energy to penetrate the window on P, and the partition separating $P_1$ and $P_2$. The energy loss measured in the counter $P_1$ and the range determined by the presence or absence of an accompanying pulse in $P_2$ is used to determine what portion of the radiation are electrons and what portion are protons or heavier particles.

Another variation of the proportional counter telescope has been devised by the University of Chicago. The counter consists of a 1-in tube, 2 inches on a side, surrounded by six others of the same size in a concentric arrangement about the center tube. The counters are filled with a 40-percent-methane-60-percent-argon gas combination under 60-cm pressure. The whole assembly

is contained in a lead shield of thickness 5 gm/cm$^2$. The center counter is connected to a pulse amplifier, in turn feeding a scaler chain. The other counters are connected in two triples to identical amplifiers. In addition to the single events counter by the center tube, triple events occurring in the center tube and any two others diametrically opposite are counted by having the three outputs connected to a triple coincidence circuit. The device will measure electrons and protons of energies greater than 12 mev and 70 mev, respectively.

The central counter may be used independently to determine the single count rate for charged particles inside the lead shielding. Thus the single counter provides a measure of the bremsstrahlung and is used as a monitor of this radiation. Figure 16 shows a schematic representation of the University of Chicago Proportional Counter Telescope.

h. Cerenkov Detectors

When a high-energy charged particle enters a medium of index of refraction greater than one, it is moving faster than the speed of light in that medium. Under these conditions radiation is produced at all wavelengths for which $\beta_n > 1$ ($\beta$ = V/C). This radiation is known as Cerenkov radiation. It is possible to make use of this effect to distinguish between electrons and protons in the radiation zones.

The main limitations on the choice of a detector is that it be a poor scintillator, be transparent in the wavelength region in which radiation is produced, and that the photomultiplier used to detect it is sensitive. Due to the different mass of electrons and protons, there is a large difference in the energy threshold for Cerenkov radiation. It is also possible to adjust to some extent the low energy threshold for electrons by biasing the output circuit to record only pulses above a certain minimum height.

The most likely configuration would use two or more detectors with different proton thresholds but biased so as to have the same electron threshold. The outputs of these detectors coupled with a counter would give a rough energy distribution for protons as well as the electron-proton abundance ratio if the proton threshold for one of the Cerenkov counters is higher than about 500 to 700 Mev, since it is not very likely that there are a large number of protons above this energy in space.

3. Internal Radiation Detectors

High-energy electrons incident on the vehicle shell will give rise to secondary radiation which penetrates to the inside of the vehicle. X-rays are generated by accelerating electrons to an appropriate energy and then allowing them to stop in material of high-atomic number. Electrons of sufficient

energy will collide with atoms of the material and release secondary electrons. A fraction of the electron energy appears as electromagnetic radiation, gamma and x-rays, called bremsstrahlung, with photon energies distributed between zero and the full energy of the electrons striking the target.

It is this secondary radiation which concerns the occupants and equipment inside the vehicle. The exposure rate in roentgens per unit time can be measured by various instruments. Among those more commonly used are cavity chambers, Geiger counters, scintillation counters, and photographic films.

a. Cavity Chamber

The most commonly used cavity chamber detector is the Victoreen condenser roentgen meter. This device consists of an air-filled nylon or bakelite chamber, coated on the inside with a conducting graphite mixture and fitted with an aluminum central electrode.

The chamber proper is mounted on a cylindrical stem which acts as a capacitor. Ionization in the air in the chamber allows charge to leak off the capacitor, and the amount of this loss, as measured by the change in voltage across the capacitor, provides a measure of the radiation exposure.

For measuring x-rays, the chamber walls are made roughly air-equivalent and the filling gas is air, so that the response is generally proportional to the exposure dose. The Victoreen chamber calibrated for conventional x-ray energies gives too low a reading on high-energy x-rays or on gamma rays of greater than 200 kev, and a separate calibration must be carried out for this energy region. When radiations of very low intensity must be measured, the more sensitive Geiger and scintillation counters have an advantage.

b. Geiger Counter

The response of a Geiger counter to x-rays is due mainly to secondary electrons generated in the walls and crossing the sensitive volume. The output of the counter is one pulse for each electron. See references 43 and 51 for more details of Geiger counters.

c. Scintillation Counter

The scintillation counters already discussed may be used to detect secondary electrons inside the vehicle. See the section on external radiation detectors.

d. Photographic Film

A charged particle passing through a grain of photographic emulsion causes changes in the emulsion when the film is developed. A blackening of the

emulsion occurs which can be measured as an increase in photographic density. In this way it is possible to detect electrons and heavy particles and, through the effects of their secondary electrons, x-rays. However, due to the time consuming procedure required to analyze emulsion plates, this method will not be discussed further in connection with the instrument requirements.

## F. Meteorite Detection

It has been previously mentioned that meteorite penetration of a sealed space vehicle poses the most hazardous event which can occur in space flight. Other meteorite events of a less hazardous nature are the constant erosion of a vehicle surface skin and the possible impact on external optical surfaces which may render these ineffective. Volumes I and II of this study cover in detail the meteorite environment and the effects of this environment on vehicles and equipment. The reader is referred to them for background on the problem.

There are many ways by which meteorites can be detected impinging upon the vehicle. It may not be required to monitor meteorite impacts but perhaps also the effects caused by these impacts. Such effects are pressure leaks caused by penetration (already covered in detail) and changes in spectral characteristics of the surface (the most important of these is the $\alpha/\epsilon$ ratio). Then again, it may be important to monitor oncoming meteorites prior to impact on the vehicle. Radio and radar detection may pose a solution along with a knowledge of the occurence of definite meteoric phenomena such as showers and comets which repeat themselves year after year. At present, meteorite detection consists of radar and astronomical ground observations and detection from rockets and satellites. The material that follows describes these rocket and satellite detection devices. The most commonly used detectors employ acoustic microphone devices, scintillation devices, and wire gages.

### 1. Acoustic Detector

Airborne components of the micrometeorite detection system (Ref. 27, 41) consist of (1) a detector (diaphragm and microphone); (2) a bandpass amplifier; and (3) two logic circuits (each with a trigger, flip-flop, and emitter follower).

The micrometeorite system is momentum sensitive, i.e., the output of the amplifier is proportional to the mass times the velocity of the impacting particle. A micrometeorite striking the diaphragm will transfer its entire momentum inelastically to the diaphragm. An acoustic pulse results which travels to the microphone. The 100-KC component of the resulting pulse is picked up by a piezoelectric crystal which rings at this frequency; the 100 KC pulse is then amplified and the envelope detected. A two-channel pulse height analyzer classifies the pulse according to whether it is produced by a low

momentum ($> \sim 5 \times 10^{-4}$ gm cm/sec)or a high momentum ($> \sim 5 \times 10^{-3}$ gm cm/sec) particle.

The diaphragm is made of aluminum (7075-ST6) painted black on the vehicle side and polished on the outer face. The microphone is attached to the black side of the diaphragm and centrally located. The size and thickness of the diaphragm depends upon the range of particle momenta to be measured to obtain a well defined acoustic pulse.

2. Scintillation Detector

Berg (Ref. 55) described in detail a scintilling type of meteorite detector. The device consists of a photo-tube (Dumont 6363) covered with two 800 A opaque aluminum coatings separated by a thin coating of silicone monoxide (SiO). The SiO coating between the aluminum coatings acts as a dielectric forming a condenser. A particle impacting the coating and not penetrating completely will convey its kinetic energy to the SiO in the form of heat. This heat will cause a change in the dielectric which in turn causes a momentary voltage drop pulse which is telemetered. A unique feature is the recovery action of the dielectric. After the heat has been dissipated the dielectric attains its normal value and is again available for use.

If a particle has sufficient mass and velocity to penetrate the dielectric coating and strikes the photo tube, the remaining kinetic energy (total minus the energy lost as heat in the dielectric) is transformed into visible light. This light is reflected to the photo-tube where the pulse is amplified. This detection method is 100 to 1000 times more sensitive than acoustic type detectors. An acoustic microphone is mounted on the side of the photo-tube and picks up the particle momentum which is correlated to the output of the dielectric and/or the photo-tube.

A cutaway view of a similar device used previously on rocket flights is shown in Figure 17. With exception of the exit window at the apex, the polished lucite cone is completely coated with an opaque layer of aluminum 800 Å thick. The window is adjacent to the photo-tube. The method of operation is similar to that described above. However, due to the long light path (in the lucite cone), Cerenkov radiation is encountered. The method described above does not encounter this problem.

3. Micrometeorite Erosion Gage

Another approach to the micrometeorite problem has been proposed by Secretan of NASA (Ref. 55). The gage is based on photoelectric principles. The penetration of an aluminized layer by the meteorites and the resulting increase in light transmitted to on especially designed cadmium sulfide photoelectric cell are related quantitatively to the number of particles and

energy. The gage is shown in Figure 18. The resistance of the cadmium sulfide cell varies exponentially with light. The advantage of this gage is that besides measuring individual impacts as pulses, it also measures the cumulative effort of the meteorite impacts. As more of the opaque surface is eroded more light is intercepted and consequently the d-c level of the voltage is increased.

4. Wire Gage

A device consisting of twelve gages has been developed by the Air Force Cambridge Research Center (Ref. 56, 57). These gages present a total of about two square inches of sensitive area and each of the twelve is sensitive to the impact of a single micrometeorite of 5 to 10 microns in diameter. The individual gages are 1 square centimeter in area and wound with two layers of enamelled wire of 17-micron diameter. This insures that the entire area is covered and is sensitive to impacts. An impact upon one of the gages destroys its electrical continuity and this is reported back by telemetry.

5. Radioactive Erosion Gage

Another method of erosion measurement utilizes the number of beta particles that are backscattered from a thin target as a direct indication of the material thickness. By observing the change in number of backscattered particles which results from the change in target thickness, it is possible to determine the rate at which a physical process is removing material from the target surface (Ref. 59). This method is extremely sensitive and most convenient for satellite application. The method is accurate, involving a digital counting operation (number of counts/second), rather than a delicate measurement of the surface property of the satellite. Figures 19 and 20 show the system and circuitry. Some of the advantages of such a device are listed below.

(1) Data is monitored periodically.

(2) No data storage is necessary.

(3) Minimum amount of information needs to be transmitted.

(4) Compatible with any telemetering system.

(5) Amount of power is extremely small (10 d-c volts at 2 ma).

(6) 1 to 2 ounces weight.

Four considerations in the choice of the radioactive emitter are:

(1) With a $\beta$-ray emitter of high energy, use a rugged counter behind the skin, because $\gamma$ rays will not be able to penetrate skin, and a $\gamma$ emitter may effect other instruments. $\beta$-particles have a limited range and would therefore only effect the counter which they are designed to operate.

(2) The half-life should not be too short, otherwise activity will decay away quite appreciably while the satellite is still in orbit (at least several days).

(3) Activity (inversely proportional to the half-life) should not be too weak; that is, half-life should not be too long otherwise too much material is required to give an appreciable counting rate. Since the cosmic ray background acting on the counter may be 10 counts per second, the $\beta$-activity should give a higher counting rate.

(4) The radioactive nucleus chosen should be compatible with the skin material and should not lead to any undesirable chemical or metallurgical problems.

Methods for incorporating the radioactive nuclei in the skin:

(1) Paint on a thin coating.

(2) Evaporation in a vacuum.

(3) Diffusion--radioactive atoms penetrate skin thickness.

(4) Prepare radioactive skin and overlay it on the base metal by rolling methods.

(5) Activate a portion of the satellite skin directly in a nuclear reactor where neutron bombardment produces radioactive atoms throughout the skin.

G. Acoustic Noise Measurement

Acoustic noise has been determined as a deleterious environment for manned space vehicles. Boundary layer noise during boost and re-entry may be as high as 140-150 db at the manned capsule. This intensity is sufficient to fatigue metals, cause malfunction of electronic components, interfere with hearing, and cause nausea and dizziness.

The devices used today for measuring such high sound pressure levels are condenser-type microphones (Ref. 67). One such device which seems applicable to the problem at hand will be discussed. Other devices incorporating semi-conductor microphones are not applicable because of their low intensity ranges (Ref. 68).

Condenser-type microphones are currently used to meaure high sound pressures of jet engine and rocket exhausts. These devices are capable of measuring levels to 214 db. The device employs a clamped plate as a diaphragm. The microphone is 0.6 inch in diameter and 0.4 inch thick making it highly attractive for boundary layer measurements. The microphone itself is limited to a temperature range to 300°F continuously. For boundary layer temperature of the order of 2000 to 3000°F during re-entry, a probe tube which threads on the end of the microphone may be used. This configuration can be used to 700°C without cooling. For higher temperatures a water cooled jacket surrounding the tube can be employed.

## SECTION III

## RECOMMENDED INSTRUMENTATION

The instruments presented below have been selected because of their special features which make them attractive for use in all vehicles.

The instruments have the required ranges, accuracies, and sensitivities for monitoring vehicle safety. Many of the devices presented here are still in the development stage, while others have proven themselves satisfactory in high-speed flight. Each sensor presented is discussed in some detail with emphasis on range, speed of response, accuracy, sensitivity, and construction.

### A. Temperature Measurement

The high temperatures to be measured eliminates many of the present conventional devices. The sensors selected here meet certain requirements for use in re-entry vehicles. For stagnation temperature measurements the Tungsten-Iridium thermocouple will provide the necessary means. For surface temperature measurements other than stagnation, a thin metal resistance thermometer has been selected.

#### 1. Tungsten-Iridium Thermocouple

Tungsten-Iridium thermocouples are capable of satisfactory performance in the 3000 to 4000$^{o}$F temperature range. The only limitation of the gage is the temperature extremes of the base metals. The only significant drawback in comparison to more conventional thermocouples is their relative instability in an oxygen environment. However, with proper insulation and protection these gages can be designed to function for lengthy periods in the re-entry environments.

The gages have been used in the steel industry for measuring the temperature of liquid steel. Temperature response of 2000 degrees in a few seconds have been obtained with the bare thermocouple. The requirements for insulation from the oxidative atmosphere will reduce the response time somewhat. It is in this area that Tungsten-Iridium thermocouples have the advantage (Ref 48). A typical output curve for this gage is shown on Figure 21. From the slope of this curve a sensitivity of $1.25 \times 10^{-2}$ mv/deg$^{o}$F is obtained.

The response time required is based on the temperature rise rate of the stagnation point. Rise rates of the order of 60$^{o}$F/sec. for stainless steel skins are anticipated for a glide re-entry. However, the response time will depend upon the gage shielding.

Several methods are available to protect the gage from corrosion and oxidation. The usual methods include gas-tight metallic or ceramic wells or tubes. In order to minimize response time the ideal method would be to make the gage an integral part of the surface material located below the surface. However, with the present state of the art this is difficult. An alternate method would be to groove the surface sufficiently, such that the gage would be just below the surface, and then cover the gage with a thin sheet of surface material, either bonded or plated. Bonding may be difficult for the temperature regimes involved. The development of suitable bonds is now in progress. Typical of currently available ceramic cements are: Corcast (Corning Glass), Ecco Ceram (Emerson Cumming), Saureisen (Saureisen Co.). These are good to 2000°F.

Another method of attachment currently under development (73), makes use of a small disk of the skin metal as one half of thermocouple junction. The disk is electrically insulated from the surrounding material by a ceramic insulator.

The accuracies of these gages is of the order of $\pm$ 5 percent, with good repeatability characteristics. Platinum gages currently have repeatability accuracies of the order of 1/2 percent. For safety instrumentation, accuracies of $\pm$ 5 percent are adequate; however, to be used as flight control sensors greater accuracy would be required.

There are many refractory materials available for thermocouple protection. The most common types are alumina ($AL_2O2$); beryllia (BeO), magnesia (MgO), thoria ($ThO_2$), zirconia ($ZrO_2$), Degussit AL23, and sapphire (monocrystalline alumina). Bell Aircraft reports that a Tungsten-Iridium thermocouple using a sapphire protector was operated for 75 hours in a 1.5 percent free oxygen atmosphere at 3452°F(Ref 11).

The problem of maintaining a reference junction temperature is another disadvantage of the thermocouple; however, this does not pose a difficult problem.

2. Thin Film Resistance Thermometer

For monitoring temperatures at critical structural regions, thin film resistance thermometers are selected because of their rapid response (on the order of microseconds), size (in the order of 1/10 micron thick), and sensitivity (temperature fluctuations of less than 1°F).

The resistance thermometer is about 75 times more sensitive than the thermocouple and the sensitivity can be varied by varying the energizing current in the film. The resistance thermometer is easier to install and does not require a reference junction or reference temperature measurement.

There are many ways to fabricate a resistance thermometer. The evaporation technique consists of mounting a metal filament between two electrodes and passing a sufficiently high current to vaporize the filament on the part to be plated. This process is performed in a near vacuum. The thickness of the coating is controlled by the distance between the filament and the part and the time interval used. Another technique employs the use of metal foil soldered to lead wires and bonded to the insulator. The advantage of this method is that the instrument can be mounted on any material and lead wires can be easily installed and ground flush with the surface before the element is installed.

A summary of construction techniques and characteristics can be seen in the Table 3. This data was obtained from the Cornell Aeronautical Laboratory (Ref 46). Platinum paint on a glass insulator proved to be the most satisfactory combination for the instrument. Temperatures in the range of 2000 to 3000°F have been measured.

The main problem to contend with in resistance thermometry is to provide a suitable bond between the insulator and the surface to be measured. Glass insulators soften above 1250°F and it is therefore necessary to obtain a suitable high temperature insulator. Fuzed quartz and pyrex glass have good working properties up to 2000°F (Ref 75).

B. Pressure Measurement

1. Dynamic Pressure Loading

The impact pressure sensor under development at Lockheed Aircraft Company (Ref 21) offers an attractive means for monitoring surface pressures on a hyper-velocity re-entry vehicle. The significant difference between this device and those commercially available is that the diaphragm is an integral part of the vehicle surface.

If a surface hole is located at the point where the pressure is to be measured and if before plating a tailored plug is inserted in the hole and plated simultaneously with the rest of the surface, except for a thin annular ring around the outside edge of the plug end, a rigid-center fixed-edge diaphragm is produced.

Good thermal contact between the plug and the diaphragm is obtained by plating. This method insures a mechanically stiff and rigid combination, resulting in small surface deflections with corresponding deformations distributed over the entire plug area.

TABLE 3

CONSTRUCTION TECHNIQUES AND CHARACTERISTICS OF THIN-FILM RESISTANCE THERMOMETERS

| Metal | Technique | Approx. Thickness | Base Material | Comments |
|---|---|---|---|---|
| Gold | Foil | 1/10 micron | Glass and Lucite | Extremely fragile-completely eroded off after 5 microseconds |
| Gold | Foil | 1 micron | " " " | " " " " " |
| Nickel | Foil | 1 micron | Lucite | Very durable-some erosion after tests, could not obtain good mechanical bond to Lucite and noisy signal was obtained |
| Nickel | Evaporative | 1/10 micron | Glass and Lucite | Fragile-major erosion during tests, difficulty in depositing on Lucite due to outgassing and difference in thermal expansion, poor bond to glass |
| Platinum | Evaporative | 1/10 micron | Glass | Fragile-major to complete erosion during tests, very poor bond to glass |
| Rhodium | Evaporative | 1/100 micron | Glass | Very durable-not tested, difficulty in calibration due to thinness and high resistance |
| Chromium | Evaporative | 1/100 micron | Glass | Same as above |
| Platinum[2] Silver alloy | Paint | 1 micron | Glass & "Lava" | Excellent durability-minor erosion during tests, excellent bond to glass, unsatisfactory on "Lava" due to "Lava" porosity, poor uniformity |
| Platinum[3] Gold alloy | Paint | 1/10 micron | Glass | Durable-some erosion during tests, good bond to glass, good uniformity |

TABLE 3 (Cont.)

| Metal | Technique | Approx. Thickness | Base Material | Comments |
|---|---|---|---|---|
| Platinum(4) | Paint | 1/10 micron | Glass | Very durable-minor erosion during tests, excellent bond to glass, excellent uniformity |

(1) All specimens were mounted on the stagnation point of a sphere and shock tunnel tested at M=5.5, stagnation temperature of about 2900°F, and an air density corresponding to about 100,000 ft. The period of uniform flow was about 2 milliseconds, followed by a flow of hot combustion gases.

(2) Hanovia Liquid Platinum Alloy #130-A

(3) Hanovia Liquid Bright Platinum #05

(4) Hanovia Liquid Bright Platinum #05-X

The resulting rigid diaphragm makes necessary a correspondingly rigid measuring device. This is required in order to minimize the energy lost in straining the diaphragm rather than the force transducer.

If the spring constant of the diaphragm is $K_D$ and that of the driving plug $K_T$, the ratio of $K_T/K_D$ should be large for maximum transducer stress and minimum dependence on diaphragm elastic properties. From Figure 22, $K_D$ can be reduced either by decreasing the plug diameter or by increasing the annular ring width. Figure 23 indicates plug deflection plotted against diameter for several annular ring widths (d).

The annular ring is a potential hot spot because the thermal conductivity at this point is small as compared to the plated areas. The wider the ring, the higher the probable temperature.

This device is capable of a sensing impact pressures to several hundred psi.

Before selecting an adequate transducer to operate with the diaphragm, the frequency of the alternating pressures must be determined. Wrathall of Lockheed has calculated the equivalent frequency from a pressure-time-history of a typical re-entry vehicle as 0.126 cps. In order to have a response error of less than 1 percent, a resonant frequency 20 times the frequency being measured is required on the basis of classical one degree of freedom system analysis or approximately a resonant frequency of 2.5 cps.

Several transducers have been studied for use with this device. Strain gages were considered inadequate because of the intolerably low spring constant and of the large deflection required by strain gages. Other devices are magnetostrictive, servo-self-balance, piezo-electric and pressure-controlled crystal oscillators.

Of all the above, the piezo-electric transducer appeared the most attractive because of the required stiffness. However, one drawback is the high shunt resistance requirements necessitating an electrometer tube which is subject to the effects of shock and vibration.

Development of more rugged tubes and possible use of transistors would lessen this problem.

The characteristics of this device are:

Range - 0 to several hundred psi.

Frequency Response - 2.25 cps.

Accuracy - 1 percent.

Sensitivity - expressed in MV per lb of force on the transducer. The higher the output the less stringent requirements for amplification.

Temperature Range - limited by the temperature of the annular ring. Usually in the range of 1000 to 2000°F. The selection of high temperature material for the diaphragm surface will ease the problem.

2. Internal-External Pressure Ratio

Internal pressures ranging from 14.7 psi down to 4.0 psi are to be monitored in conjunction with external pressures of less than $10^{-11}$ mm Hg at great distances from the earth. Pressure ratios on the order of $10^{12}$ or more are to be experienced.

a. Internal-Pressure Sensor

In order to detect leak-rates an extremely sensitive gage is required. In order to detect an internal pressure drop of 0.10 psi a response time of 63.2 percent of 34.2 sec is required. This amounts to 21.6 sec or 0.005 psi/sec (0.254 mm Hg/sec).

The Haven's Cyclic Pressure Gage will satisfy the requirements for internal pressure monitoring. This gage is attractive for several reasons. The gage not only covers the complete range of pressures from atmospheric down to less than $10^{-5}$ mm Hg, but is rugged, has a small volume, and requires little attention for high accuracy of measurement.

The gage works on the principle that an a-c signal can be obtained from a normally d-c pressure gauge by cyclically changing the pressure at a given frequency. An a-c signal is developed which is primarily a function of pressure alone, as long as the electrical signal from the gage is appreciably above thermal and microphonic noise (Ref 14).

Figure 24 is a schematic diagram of the cyclic gage. Resistance wires are used as detecting elements and bellows are employed to change the pressure. The detecting elements in the gage are each placed inside a sylphon brass bellows, 6 cc in volume. The eccentric shaft of a small motor drives both bellows, changing their volumes by about 20 percent. With this double bellows arrangement, the shaft is working against the same pressure in each of the bellows independently of the pressure surrounding the gage. The pressure is communicated to the element inside the bellows through small holes, one of 1-mm diameter and the other of 1/2-mm diameter, which restrict the flow of gas.

At pressures higher than 50 mm Hg, the tungsten wire acts as a simple thermal element. At these pressures the temperature, and correspondingly the resistance, of the wire increases when the gas in the bellows gives up

heat under compression, and decreases when the gas expands. The temperature change of the wire is a function of the mass of gas in the bellows and hence of the pressure.

This gage measures pressure changes directly and is independent of gas composition. It has a range of $10^{-5}$ to $10^{3}$ mm Hg with an accuracy of 5 percent. The device weighs one lb., has a volume of 20 cubic inches, and requires 50 watts of power (Ref 11).

b. External Pressure Gage

To continuously monitor space vacuum there are numerous devices which will satisfy the requirements of range, response, accuracy and sensitivity. Such gages as the radioactive ionization gage (alphatron) and the Bayard-Alpert ionization gage are capable of pressure readings below $10^{-8}$ mm Hg with the latter capable of attaining $10^{-11}$ mm Hg. Each of these gages is described in detail in the literature. Each is dependent upon the gas composition for pressure measurement.

A modified cyclic gage, using a Bayard-Alpert ionization gage as the pressure-sensitive element in the bellows, permits measurements of pressures down to $10^{-11}$ mm Hg.

The ionization gage has an accuracy of 2% and requires 20 to 30 watts power. Ionization gages weigh about one-half pound and occupy from 10 to 20 cubic inches. These have been successfully used in high-altitude rockets.

C. Strain Measurement

The idea of continuously monitoring the state of strain of critical structural members seems very attractive. Strain gages could be used to obtain the combined structural strain due to several factors such as aerodynamic loads, thermal gradients, acceleration and vibration.

Although the state of the art of strain gage instrumentation is fairly advanced there are important reasons that have limited their use almost exclusively to laboratory and research type applications. These reasons are as follows.

Installations problems are present, such as bonding to the structure to insure that there is no slippage between gage and the material so that the strain is transferred exactly in both magnitude and direction to the gage. In addition, the electrical insulation qualities of the bond must not change significantly with humidity and temperature.

Although the circuit problems due in the main to the small electrical signals and d-c circuitry have been solved quite successfully for laboratory and

limited flight tests, the application to field type testing requires further development.

The application to indeterminate structures requires complex analysis to determine the maximum strain from the indication of several gages. The use of computers is indicated for in-flight strain monitoring.

By far the most serious problem is temperature sensitivity which is very difficult to compensate for in the case of transient temperatures.

Despite the above disadvantages strain gages should be used on a limited basis, such as verification of design of some structural part or in an area shielded from the extreme temperature. In addition, the member to which the strain gage is attached can be made statically determinate to reduce the complexity of analysis.

These modifications both in shielding and method of attachment can be related either by analysis or test to the stress at an exposed point on the structure. It is therefore recommended that strain gages be considered for in-flight monitoring on a limited basis, for design verification, and possible operational use.

D. Vibration and Acceleration Measurement

Vibratory accelerations caused by boundary layer and power plant noise can be monitored by using any of the linear accelerometers presented in the state of the art. Continuously applied acceleration during the boost or re-entry phases can be continuously monitored by the vehicle guidance system. Therefore, vehicle acceleration instrumentation will not be required.

The versatility of design and application indicate that the compression type piezo-electric crystal accelerometers are most attractive for use in vehicles. Vibration frequencies up to 4000 cps demand an instrument which has a natural frequency of at least 10 KC. These types of accelerometers satisfy this requirement in small size and mass. Sensitivity of crystal accelerometers is expressed in millivolts per g (mv/g) and will vary with the impedance of the connecting cable between the instrument and its cathode follower. Sensitivities of the order of 1 to 50 mv/g are common with an accuracy of $\pm$ 5 percent. Acceleration ranges varying from . 02 to 40, 000 g are available with natural frequencies to 150 KC. Frequency response of one cps to 15 KC is typical.

The application of high-temperature materials make the crystal accelerometer capable of operating at temperatures about 500°F continuously. Special cooling methods such as water jackets increase the range to well above 500°F which is the requirement for structural vibration measurements with temperature sensitivities below $\pm$ 10 percent.

These devices vary in weight from 1 gram to 60 grams and occupy a volume of a fraction of a cubic inch to several cubic inches. No external power is required for the sensor due to its self-generating voltage characteristics (piezo-electric); however, power requirements for the associated electronics (cathode follower and amplifier) is of the order of 1 watt or less.

A typical sub-miniature piezo-electric accelerometer commercially available uses a Lead Zirconate Crystal and has a weight of 1 gram, sensitivity of 2 mv/g, and range .5 to 40,000 g, output impedance 1600 megohms shunted by .004 mfd.

E. Radiation Measurement

The vehicle should have radiation detectors and integrators which will indicate the total dose received inside the vehicle. A battery of detectors will be necessary for various types of particles and various energy ranges of the particles. The battery of detectors will be made up of scintillation counters, ionization chambers, Geiger counters, and proportional counter telescopes.

The scintillation counter measures the total flux of electrons of energy greater than 225 kev and protons of energy greater than 2 mev. The detector is a plastic cylinder 2.5 centimeters in diameter and 0.64 centimeters thick. Light pulses are detected with a photomultiplier tube. The detector is surrounded by 10 $mg/cm^2$ of aluminum. There is a 5-centimeter aluminum window in the side of the vehicle, also 10 $mg/cm^2$ thick. To decrease noise in the output, the scaling circuit is biased to accept pulses equivalent to an energy loss in the plastic of at least 200 kev. The alumium window subtends a solid angle of about 0.5 steradian at the detector. Data are recorded and transmitted in both analog and digital form.

An integrating type ionization chamber and a Geiger counter are used to measure 1.25 mev electrons or 25 mev protons or greater. The ion chamber consists of a 3-inch sphere filled with argon gas to an absolute pressure of approximately 6 atmospheres. The ions are collected by a quartz rod, the upper end of which is coated. The central rod collects electrons formed by ionizing radiation in the argon gas of the chamber.

The second detector is a small halogen geiger counter. The counting rate is recorded in digital and analog form. Neither the ion chamber nor the geiger counter are deliberately shielded. The shields encountered by the incident radiation are the vehicle walls, and aluminum can surrounding the detectors, the walls of the detectors, and the other apparatus present in the vehicle.

The proportional counter telescope measures high energy charged particles in the presence of strong bremsstrahlung. The apparatus is composed of a triple coincidence counter system surrounded by 5 $gm/cm^2$ of lead.

The apparatus consists of seven cylindrical proportional counters, six in a concentric ring around the seventh, with the outer counters connected in two adjacent groups of three. The pulses from each group of counters are first amplified before entering the triple coincidence circuit. The central counter, which forms the second counter of the triple coincidence, is also used to determine the single counter count rate for charged particles inside the lead shielding. Thus the single counter provides a measure of the bremsstrahlung and is used as a monitor of this radiation, in addition to providing the single count rate needed for corrections of accidentals at very high levels of flux. The output of the single counter is also fed to a scaling circuit.

The minimum energy required to penetrate the coincidence counter with shielding is 70 mev for protons and 12 mev for electrons. Thus only relativistic electrons will be measured as triple coincidence events and only protons in excess of 70 mev will be registered.

Each of the detectors measures the integrated flux of particles above its energy cutoff. However, due to the different shielding used, each has a different cutoff as shown below.

| Detector | Detection Threshold (mev) | |
|---|---|---|
| | Electrons | Protons |
| Scintillation Counter | 0.225 | 2.0 |
| Geiger Counter-Ionization Chamber | 1.25 | 25.0 |
| Proportional Counter-Telescope | 12.0 | 70.0 |

The first detector has a weight of about 4.5 pounds including the auxiliary scaling, counting and indicating equipment. The detector itself weighs about 1 pound and requires 500 to 1000 volts d-c power.

The second detector set weighs about 2 pounds and requires 300 volts or more for the ionization chamber and 500 volts or more for the geiger counter.

The third detector weighs about 5 1/4 pounds and requires about 1000 volts d-c power.

The counters will be able to indicate accurately the radiation rate contributed by protons and electrons of various energies. The various radiation rates are summed and continuously integrated, giving the total dose received inside the vehicle at any time since the beginning of the space voyage.

F. Meteorite Detection Instrument tion

The problem of monitoring the effects of the meteoritic particles involves the measurement of particle size and speed, damage caused, and location of damage on vehicle surface.

A method for detection and identification of individual particle sizes and velocities is under development. At present, only the momentum (mass x velocity) of meteoritic particles can be detected. This is accomplished by acoustic microphone devices mounted on the vehicle surface. Further development of the scintillation type detector coupled to an acoustic detector will result in a device which will yield particle mass and velocity. The output of the scintillator is proportional to $Mv^2$ whereas the acoustic detector output is proportional to Mv. Having these two values, M and v can be obtained for each particle impact.

The scintillating detector proposed by Berg at NRL incorporates an acoustic microphone and gives simultaneous readings of particle energy and momentum. An unique advantage of this device is the recovery of the scintillating surface allowing the device to be used over and over. One drawback is that for a fairly large particle, i.e. one capable of penetrating the vehicle, the device may be shattered and rendered useless.

For the larger particles a combination of acoustic microphone and pressure gage detector will be used to locate a penetration into a pressurized vehicle. Compartmenting of vehicles with strategically located acoustic detectors and leak detectors will ease the problem.

The acoustic detection method has great sensitivity and measures a large area when the crystal is placed in contact with a metal surface. Sensitivity decreases with impact distance from the microphone. Signal strength is proportional to particle momentum. The constant of proportionality is determined for each individual microphone.

The transducer consists of a single piezo-electric crystal of cylindrical shape and mounted in a machined support such that the overall vibration resonances are tuned to an ultrasonic frequency at 100 KC/sec. The electrical pulse from the transducer passes through three stages of amplification. The output pulse is rectified and matched to the telemetry system. A sub-carrier oscillator is modulated at a rate dependent only on the rate of impacts.

In this manner vibrations due to particle impact are transmitted along and through the vehicle surface to the crystal detector. Impacting momentum triggers a multivibrator. The greater the distance from the microphone the greater the momentum necessary to trigger the vibrator.

The total power requirements for such a device is low, on the order of a watt or so. The weight is less than a pound with sizes determined by the

sensitivity required. Typical size of the diaphragm is 12 inches long 4 inches wide which was used on the Pioneer space probes. The diaphragm can be curved to fit the vehicle surface contour.

The use of meteorite detectors for vehicle safety is impractical within the present state of the art. This is due to the vast uncertainty in the meteorite environment and the infancy of detector development. What is needed is a system integrated with the vehicle structure which will locate an impact, determine the properties of the impacting particle and assess the damage caused. At present in order to fulfill these requirements an impractical number of detectors of various sizes, shapes, sensitivities, etc. would be required. Therefore, the recommendations for meteorite detection devices is left open pending further development in the state of the art.

Surface erosion caused by particle impacts can be monitored continuously with an erosion gauge such as described in the state-of-the art.

G. Acoustic Noise Measurement

The device most appealing for measurement of boundary layer and booster noise is the condenser microphone. A complete analysis and description can be found in Reference 67. This device has been designed to provide a rugged instrument to measure high sound pressures. The application of condenser microphones dictates low distortion, stable construction, use of materials having special physical properties, appropriate electrical circuits, and accurate individual calibration.

A detailed drawing of the microphone is shown in Figure 25. In brief, the microphone is 0.6 in. in diameter and 0.40 in. thick. It is constructed of stainless steel and glass compounds. The device is unique in the fact that it employs a clamped glass plate as a diaphragm. Thicknesses of the diaphragm varies between 0.0004 to 0.013 inch depending on required sensitivity. The device works on the principle of conversion of mechanical to electrical energy via an electrostatic field.

As the voltage developed by the condenser microphone is proportional to the amplitude of motion of the diaphragm, it is required that the diaphragm be stiffness-controlled to produce an output independent of frequency. Diaphragm resonance is damped by the resistance of the thin air space between the diaphragm and back plate, the space between diaphragm and sintered bronze sound entrance, and the resistance of the sintered bronze filter itself.

The device has a range up to 214 db with four interchangeable microphones. Sensitivity varies 1 volt depending upon the microphone. Figure 26 shows open circuit sensitivity curves for four types of microphones (Ref 67).

Axial acceleration of the mass of the diaphragm causes it to deflect to an extent proportional to the density and inversely proportional to the square of the diaphragm thickness. Expressed in equivalent sound pressure level, the sensitivity of the microphone to axial sinusoidal acceleration having a peak value of 1g is 99 db for range up to 164 db and 109 db for range up to 214 db.

Distortion is less than 5 percent up to 15 KC. The microphones have been found to withstand shock waves 20 db above their rated linear output.

Temperature limitations of the devices are imposed by the physical properties of the cable insulation. The long-time temperature exposure is limited to 300°F. For use at continuous high temperatures a probe tube which threads on the end of the microphone may be used to provide a point source pickup. By using a heat shield between the source and the microphone, temperatures as high as 1400°F have been withstood. By surrounding the probe tube with a cooling jacket, higher temperatures may be tolerated.

The associated electronics consists of a cathode follower serving as an impedance transformer due to the high impedance of the condenser microphone, a power supply, and amplifier.

## SECTION IV

## CONCLUSIONS

The work done so far leads to the conclusion that more elaborate instrumentation will be required in the future to safeguard the space vehicles against extreme environmental hazards such as excessive loadings, vibration, temperature, radiation doses, and micrometeorite impacts. It is therefore suggested that those recommended sensors having the required ranges, sensitivity and accuracy be used to monitor the above environments.

However, merely adding a few transducers will not solve the problem. What is required is a system which will continuously monitor the safety of the vehicle. This will consist of appropriate transducers integrated with the structure in such a manner that the effects of the environment can be readily sensed and that extraneous and spurious effects are minimized and have electrical outputs that are compatible with required computation.

A computer as shown in Figure 27, will perform the necessary operations on the electrical outputs of the transducers such as differentiation to determine the rate of change of a variable to predict tendencies, integration to determine the cumulative effects, signal conditioning, and comparison against predetermined values to determine safe levels. The output of the computer could be either displayed to the pilot or telemetered to the ground stations as required.

The computer can also initiate escape procedures directly in case of extreme emergency such as decompression by meteorite impact. The escape system can also be activated by the pilot when the situation is not too serious.

The relationship between safety instrumentation and control instrumentation has to be considered next.

By control instrumentation we mean such sensors as gyros, accelerometers, air data transducers and the associate computers. The safety instrumentation will form a separate system although there will be a certain amount of overlap, e. g., a single transducer can furnish data that can be used both for control and safety and can supply inputs to both systems. At the output end of the two systems the computers will also be linked, so that under certain conditions the safety computer can override the control computer. With the exception of the above, the work on the environmental safety system can procede independently.

This program is quite realistic and most of the problems can be solved by the application of state of the art techniques. Some problems can be simplified by using a systems approach. An example of this is strain measurement by incorporating appropriate design of some members of the structure as part of the instrumentation system, so that strain can be easily determined.

Table 4 shows the environmental parameters that will be monitored during the various mission phases. These include radiation, pressure, vibration, temperature, strains and micrometeorite impacts. A simplified block diagram of the proposed system is shown in Figure 27. The output of the computer is fed to the displays for the pilot's information and to the automatic control system to initiate corrective actions in situations that do not require the pilot's action and to the ground station through a telemetering link.

## FUTURE WORK

Some fruitful areas of future work would be the following:

(1) Continuation of the study of the effects of the environments on space vehicles to those environments generated by novel propulsion units such as nuclear fission rockets, thermonuclear engines, plasma jets, etc. The effect that these environments may have on the vehicle and subsystems as well as possible means of monitoring these environments should also be investigated.

(2) In the area of monitoring instrumentation a fruitful area would be to continue the study to the point of generating design specifications in conjunction with a vehicle projected for the near future, such as Dyna-Soar, where requirements are better defined.

(3) Study of environments created by defensive measures in space and high altitude vehicles employing conventional and nuclear weapons.

(4) Instrumentation for (a) space environment simulation facilities and (b) flight testing of space vehicles and satellites.

TABLE 4

ENVIRONMENTAL PARAMETERS MEASURED DURING MISSION PHASES

| Mission Phase | Concern | Environmental Parameter Measured | Quantity Controlled |
|---|---|---|---|
| Blast off | Pilot Safety | Acoustic Noise, Vibration | Exhaust Deflection |
| Boost | Pilot Safety | Vibration, Acceleration Temp., Shock, Aerodynamic Noise. | Thrust, acoustic absorption and vibration, damping and/or isolation |
| Orbit | Pilot & System Safety | Temp., press., radiation, micrometeorites | Flight path. Internal press. and cooling system. |
| Re-entry | Pilot Safety | Aerodynamic heating, dynamic press., vibration, acoustic noise, | Speed, angle of attack |
| Landing | Pilot Safety | Shock | |
| Luner | Pilot & Vehicle Safety | Atmospheric gases and pressure; Landing shock; Lunar dust consistency & Depth, Radiation, etc. | |

## APPENDIX A

## BIBLIOGRAPHY


1. Hebeler, Henry, K. and Richard D. White, "Some Design Aspects of an Interplanetary Exploratory Vehicle," Astronautical Sciences Review, April-June/1959.

2. Webb, Paul, M.D., "Protection of Man Against Transient Exposure to High Heat Loads," Advances in Astronautical Sciences, Volume 4, Plennum Press, Inc. 1959.

3. Hoover, George W., "The Man-Machine System in Space Vehicles," Advances in Astronautical Sciences, Volume 4, Plennum Press, Inc. 1959.

4. McLennan, Miles A., "Physiological Telemetry," Advances in Astronautical Sciences, Vol. 4, 1959.

5. Freundlich, Martin M., and Arthur D. Robertson, "Lubrication Problems in Space Vehicles," Advances in Astronautical Sciences, Vol. 4, 1959.

6. "Space in Human Flight," Aeronautical Engineering Review, March 1958.

7. Eggers, Alfred J., Jr. et al "Some General Considerations of the Heating of Satellites," Transactions of the ASME, Series C, November 1959.

8. Fisher, J.H. and W.R. Menetrey, "Power in Space," Mechanical Engineering, Vol. 81, No. 11, November 1959.

9. Spencer, N.W., & W.G. Dow, "Density-gage Methods for Measuring Upper-Air Temperature, Pressure and Winds, "Rocket Exploration of the Upper Atmosphere, Pergamon Press 1954.

10. Sicinski, H.S. et al, "Pressure and Density Measurements Through Partial Pressures of Atmospheric Components at Minimum Satellite Altitudes," Scientific Uses of Earth Satellites, ed. J.A. Van Allen, 1956.

11. "A Study of Flight Instrumentation for Vehicles Operating in the Fringe of, or Outside of the Earth's Atmosphere, Vol. IV Investigation of Sensing Techniques," Bell Aircraft Report No. 60009-001, under Contract No. AF33-(616)-5943. WADC TN 59-567, Vol IV, Part III.

12. Dessler, A.J., et al, "A New Instrument for Measuring Atmospheric Density and Temperature at Satellite Altitudes," Jet Propulsion, December 1958.

13. "Mach 1-10 Sensor for Re-entry Angles and Pressure," Space/Aeronautics, February 1959.

14. Havens, R., et al "A New Vacuum Gage," Review of Scientific Instruments, July, 1950.

15. Dube, F.R., et al, "Evacuation Aspects and Allied Problems in Hyper-Environmental Test Chambers," 1959 Proceedings of the IES.

16. Hansen, C.F., "Some Characteristics of the Upper Atmosphere Pertaining to Hypervelocity Flight," ARS Reprint 458-57, June 1957.

17. Dickey, F.L., and G.H. Knipp, "Sealed Cabin Reliability as Related to Structure and Internal Atmosphere," ARS Journal, September 1959.

18. Lion, Kurt, S. "Instrumentation in Scientific Research," Chap. 1-5, McGraw-Hill, 1959.

19. Liu, F.F. and T.W. Berwin, "Recent Advances in Dynamic Pressure Measurement Techniques," ARS Journal, February, 1958.

20. Spencer, N.W. & R.L. Boggess, "A Radioactive Ionization Gage Pressure Measurement System," ARS Journal, January 1959.

21. Wrathall, Taft, "Measuring Impact Pressures of Re-entering Missile Nose Cones," ISA Journal, Vol. 6, No. 10, October 1959 Page 54.

22. Li, Dr. Yao Tzu, "Pressure Transducers for Missile Testing and Control," ISA Journal, Vol. 5, No. 11, November 1958.

23. Echenrode, Robert T., and Howard A. Kirshner, "Measurement of Pressure Transients," Review of Scientific Instruments, Vol. 25, No. 1 January 1954 Page 33.

24. "Pressure-Pickup," Review of Scientific Instruments, Vol. 25, 1954 Page 411.

25. Hernandez, J.S., "A Guide to Transducer Selection," Electrical Design News, February 1960, pp. 60-74.

26. Webber, W.R., "New Determination of the Intensities of Primary Cosmic Ray Alpha Particles and Li, Be, B Nuclei at $\lambda = 41.50$ Using a Cerenkov Detector," Il Nuovo Cimento, Series X, Vol. 4 pp 1285-1306, December 1956.

27. "The Scientific Objectives of the Able-3 Program," Space Technology Laboratory, 25 May 1959.

28. Anderson, H. and H. V. Neher, "Objectives and Preliminary Design of an Integrating Ionization Chamber for a Cosmic Ray Experiment," Jet Propulsion Laboratory, May 13, 1959.

29. Rosen, Alan, et al, "Ionizing Radiation Detected by Pioneer II," Space Technology Laboratory, 6 May 1959.

30. Freden, Stanley C. and R. S. White, "Protons in the Earth's Magnetic Field," University of California Radiation Laboratory, UCRL-5581-T, May 26, 1959.

31. Josias, Conrad, "Pioneer's Radiation-Detection Instrument," Astronautics, July 1959.

32. Lindner, John W., "Exploration of the Terrestrial Radiation Belt," Space Technology Laboratory, TR-59-0000-00625, 15 June 1959.

33. Bond, Angus F., et al, "Methods of Predicting Radiation Dosage in Space Flight," American Astronautical Society Reprint No. 60-21, Jan 1960.

34. Babinsky, Andrew D., et al, "The Radiation Problem in Low Thrust Space Travel," ARS Reprint 989-54 November 1959.

35. Van Allen, J.A., "On the Radiation Hazards of Space Flight," State University of Iowa, SUI-59-7, May 1959.

36. Rosen, Alan, "Soft Radiation Measurements on Explorer VI Earth Satellite," Space Technology Laboratory. (Nov. 1959).

37. Atkinson, John H. and Victor Perez-Mendez, "Gas Cerenkov Counters," Review of Scientific Instruments, October 1959.

38. Ludwig, George H., "Cosmic-Ray Instrumentation in the First U.S. Earth Satellite," Review of Scientific Instruments, April 1959.

39. Brackmann, R. T., et al "Iodine-Vapor-Filled Ultraviolet Photon Counter," Review of Scientific Instruments, February 1958.

40. Wagner, E. B. and G. S. Hurst, "Advances in the Standard Proportional Counter Method of Fast Neutron Dosimetry," Review of Scientific Instruments February 1958.

41. 1958 NASA/USAF Space Probes (ABLE-1) Final Report Vol. 1, Summary; Vol. 2, Payload and Experiments, by Space Technology Laboratories NASA Memo 5-25-59W, June 1959.

42. Symposium on Scientific Effects of Artifically Introduced Radiations at High Altitudes, IGY Satellite Report Series, No. 9, 15 September 1959.

43. Corson, Dale R., and Robert R. Wilson, "Particle and Quantum Counters," Review of Scientific Instruments, Vol. 19, No. 4, April 1948.

44. Konecci, Eugene B., "Decompression Events in Biosatellites" ARS Preprint No. 638-58, June 1958.

45. Whipple, F. L., "Meteoritic Risk to Space Vehicles," ARS Preprint No. 499-57 October 1957.

46. Vidal, Robert J., "A Resistance Thermometer for Transient Surface Measurements," Cornell Aero. Lab., Inc., Presented at the ARS Meeting September 24-26, 1956, Buffalo, New York.

47. Methods of Experimental Physics, Vol. 1-Classical Methods, ed. Immanuel Estermann, Academic Press 1959.

48. Lampert, S. et al "A Study of Requirements for In-Flight Structural Date for Missiles and Space Vehicles, Parts I and II," WADC TR-59-478, August 1959 (Secret).

49. Davis, Leo R., "Electronics Required for Vertical Probe Radiation Package," NASA Space Science Laboratory, 19 January 1958.

50. Whyte, G.A. Principles of Radiation Dosimetry, John Wiley & Sons, Inc. 1959.

51. Ives, Ronald L., "Geiger Radiation Monitor Indicates Continuously," Electronics, October 24, 1958.

52. "Nuclear Instrumentation," Reference Data for Radio Engineers, 4th edition ITT Corporation.

53. Singer, S. F., "Measurement of Interplanetary Dust," Scientific Uses of Earth Satellites, ed. J. A. Van Allen, 1956.

54. Dubin, Maurice, "Meteoric Bombardment," Scientific Uses of Earth Satellites, ed J. A. Van Allen, 1956.

55. E. Manring and M. Dubin, "Satellite Micrometeorite Measurements," IGY Satellite Report Series, Number 3, May 1, 1958.

56. Singer, S. F., "The Effect of Meteoritic Particles on a Satellite," Jet Propulsion, Vol. 26, No. 12, December 1956.

57. Goettelman, R. C., "Measurement of Satellite Erosion Rates by the Backscattering of Beta-Rays," Jet Propulsion, Vol. 28, No. 11, November 1958.

58. Bingham, C. R., "Temperature Transducers," Electronics, July 10, 1959.

59. Barber, J. A., "Environmental Testing to 2000°F," Proceedings of the Institute of Environmental Sciences, 1959 Annual Meeting.

60. Manson, S. S., "Thermal Stresses in Design-Strain-Gage Measurements," Machine Design, October 29, 1959.

61. Beckman, Paul, and Herbert Yanowitz, "Strain Gages for Higher Temperature Measurements," Space/Aeronautics, August 1959.

62. Manson S. S., "Thermal Stresses in Design-Strain Gage Applications," Machine Design, November 1959.

63. Manson, S. S., "Thermal Stresses in Design-Measurements by Photoelasticity," Machine Design, November 26, 1959.

64. Romig, Mary F., "Stagnation Point Heat Transfer for Hypersonic Reentry," Aviation Age R&D Handbook, 1958-1959.

65. Allen, H. Julian, and A. J. Eggers, Jr., "A Study of the Motion and Aerodynamic Heating of Missiles Entering the Earth's Atmosphere at High Supersonic Speeds," NACA TN 4047, October 1957.

66. Jurgen, Ronald K., "How Transducers Measure and Control," Electronics-Engineering Edition, Vol. 31, No. 27, July 4, 1958.

67. Hilliard, John K., and Walter T. Fiola, "Condenser Microphones for Measurement of High Sound Pressures," Journ. Acoust. Soc. Amer., Vol. 29, No. 2, February 1957.

68. Burns, Fred P., "Piezoresistive Semiconductor Microphone," Journ. Acoust. Soc. Amer., Vol. 29, No. 2 February, 1957.

69. Giedt, R. R., "Vibration Measurements and Their Meaning," ARS Preprint 619-58.

70. Schalkowsky, Samuel and Henry F. Blazek, "The Rotating Pendulum Accelerometer, ARS Preprint 915-59.

71. Barr, G. M. and S. C. Morrison, "Measurements of the Vibration Environment in a Supersonic Liquid-Propellant Rocket Sled," ARS Preprint 416-57.

72. Barbiere, Robert E., and Wayne Hall, "Electronic Designer's Shock and Vibration Guide for Airborne Applications," WADC TR 58-363, December 1958.

73. Giedt, W.H., "Temperature Measurement in Solids," Product Engineering, July 21, 1958.

74. Danisheuskii, S.K., "The Immersion of Thermocouples," Industrial Laboratory, Soviet Instrumentation and Control Translation Series, Vol. 24, No. 12, December 1958.

75. Jastzebski, Zbigniew D., "Nature and Properties of Engineering Materials," John Wiley & Sons, Inc. 1959.

76. Hoge, Harold J., "Temperature Measurement in Engineering," in Temperature - Its Measurement and Control in Science and Industry, Vol. 2, ed Hugh C. Wolfe, American Institute of Physics, 1955.

77. Dubin, Maurice, et al "Calibration of Micrometeoritic Detectors Used on Satellites and Rockets," GRD, Air Force Cambridge Research Center, 1959.

# APPENDIX B

# ILLUSTRATIONS

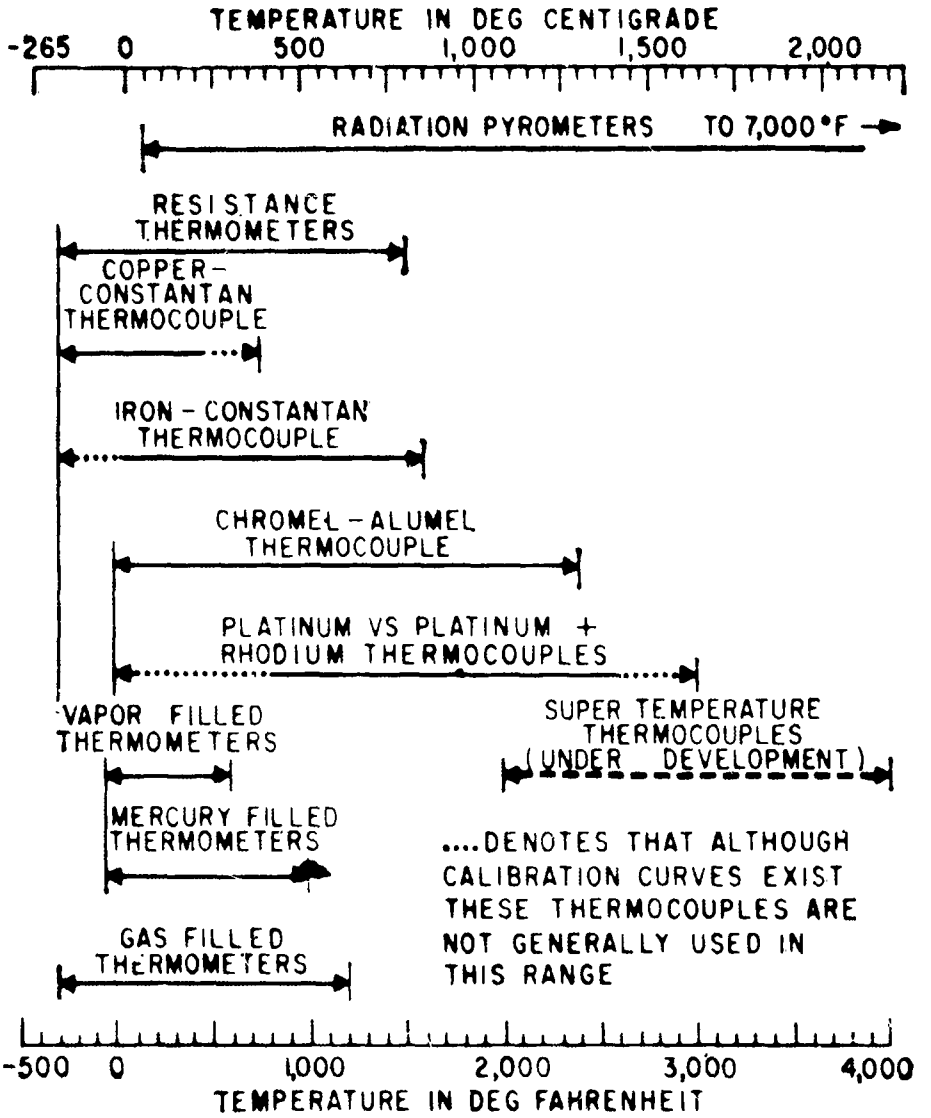


Figure 1. Normal Temperature Ranges of Transducers Which Will Provide Proportional Signals To Remote Instrumentation

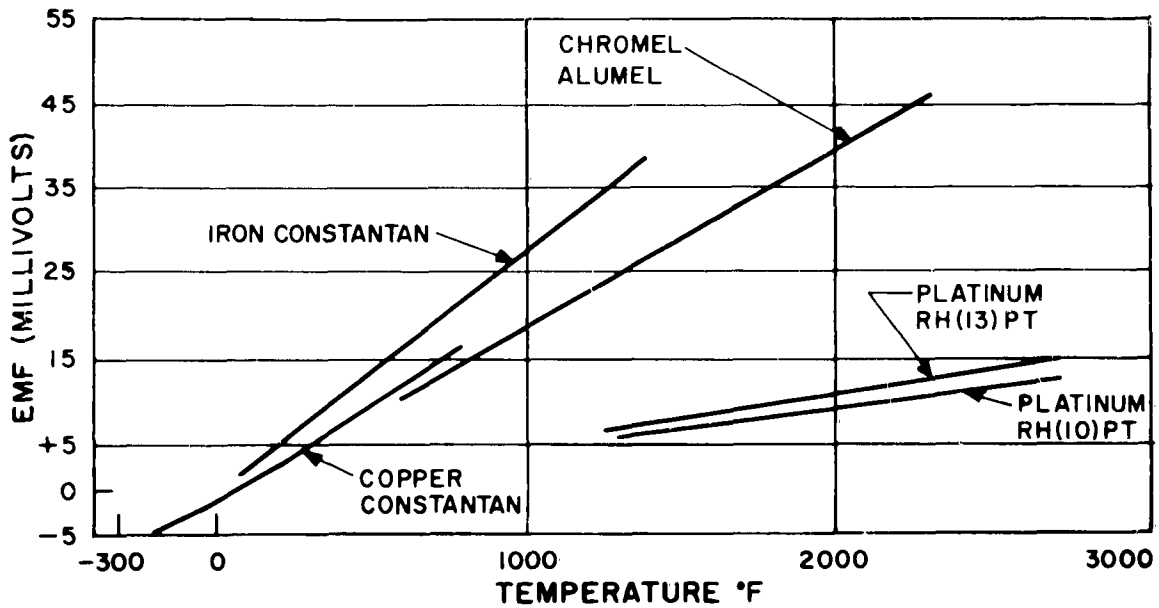


Figure 2. Thermovouple EMF Vs Temperature

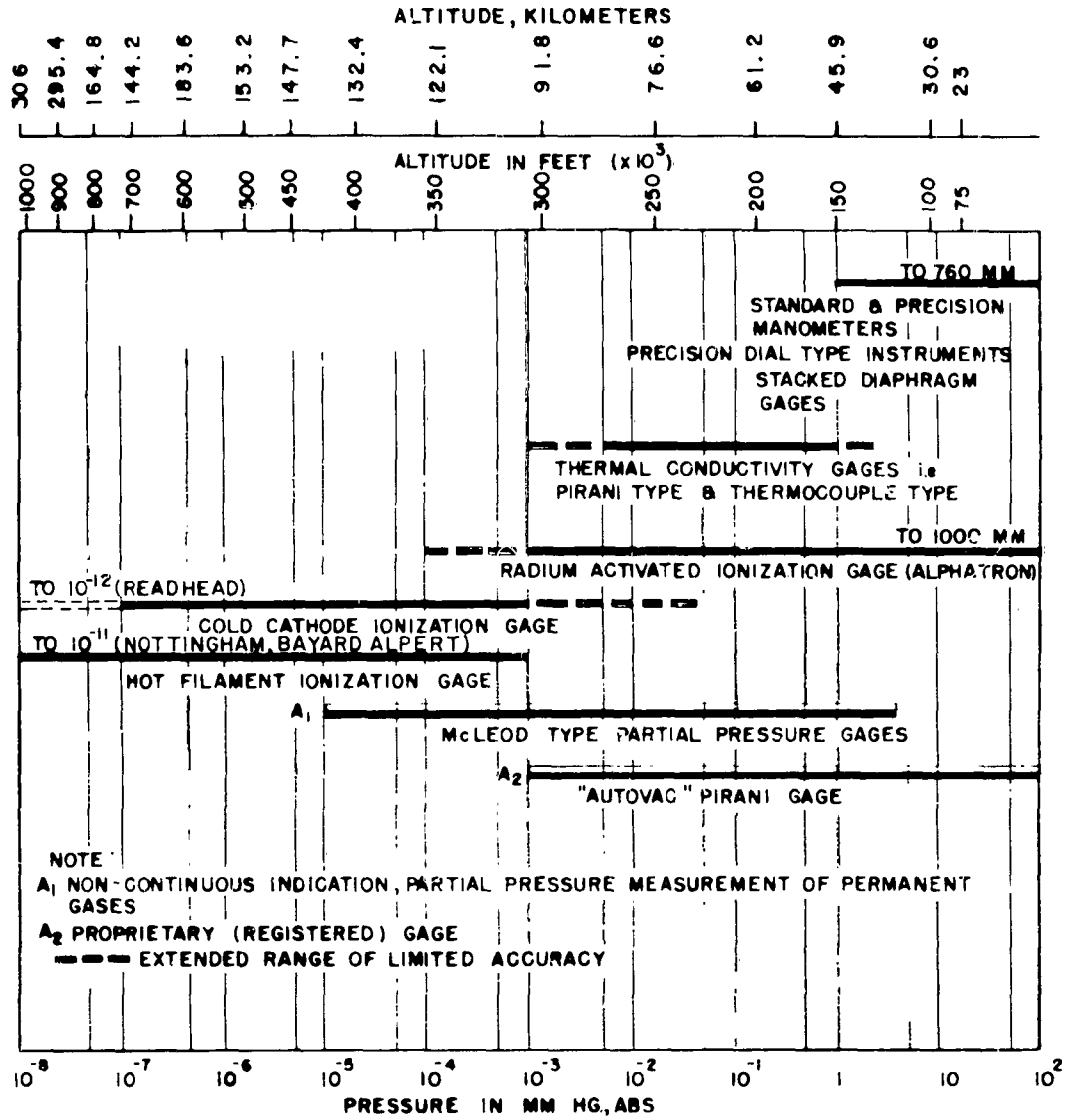


Figure 3. Useful Pressure Ranges of Vacuum Measuring Instrumentation

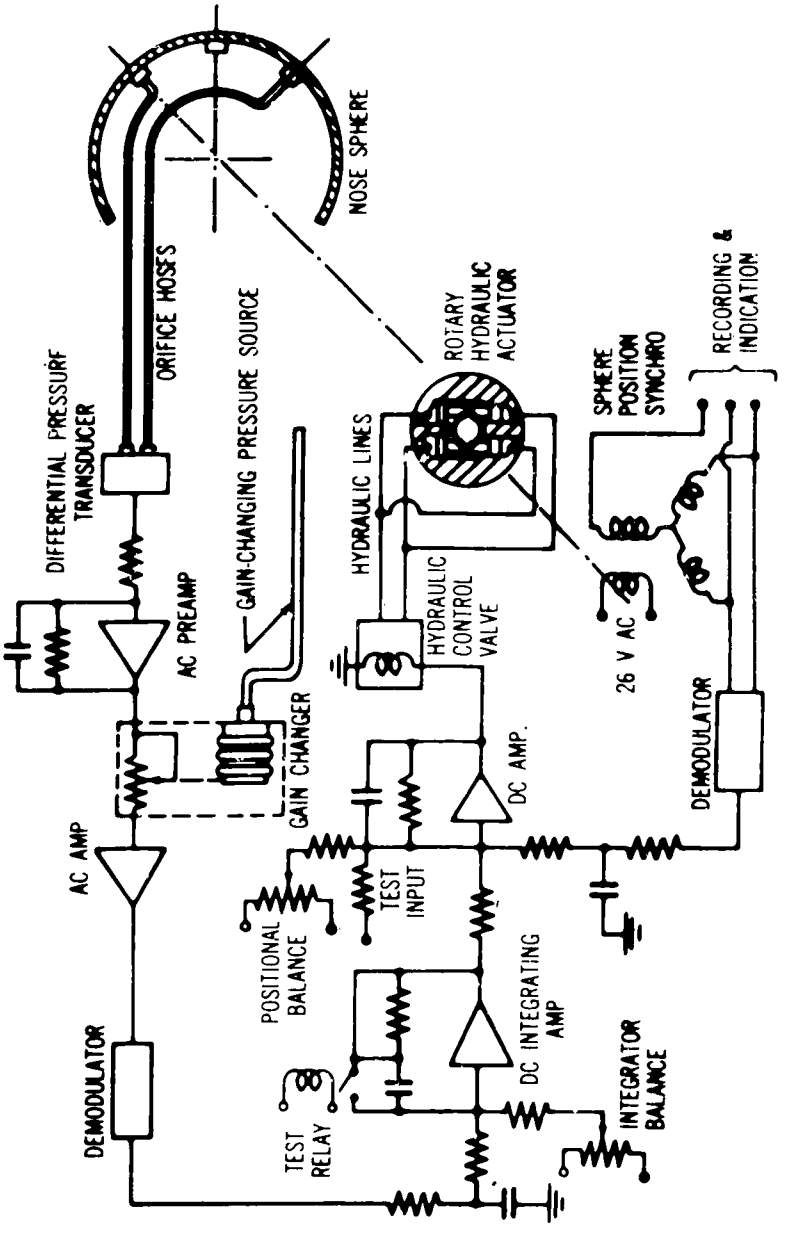


Figure 4. Q-Ball Functional Diagram

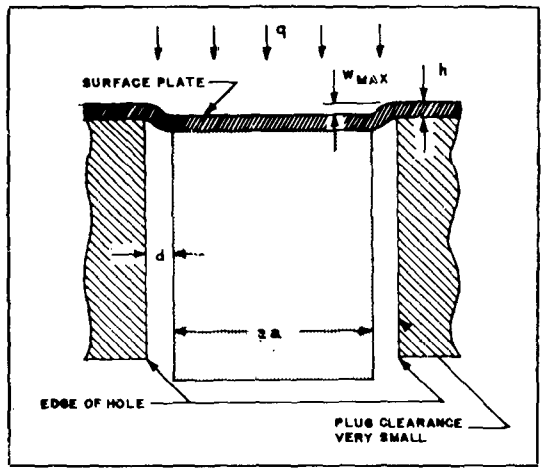


(2a = surface hole diam.; d = width unplated annular ring; h = plating thickness; $W_{max}$ = plug deflection due to pressure q.)

Figure 5. Pressure Diaphragm Formed of the Nose Cone Plating

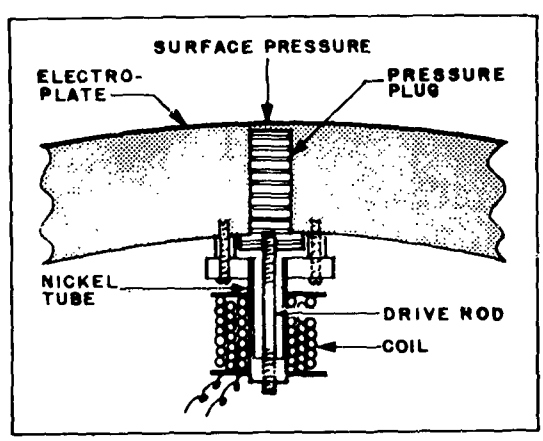


Figure 6. Magnetostrictive Pressure Transducer

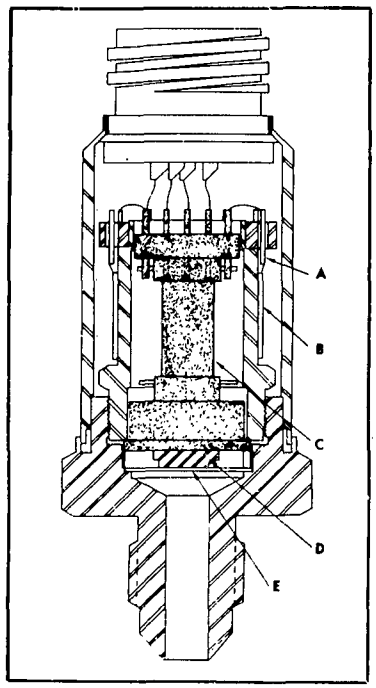


A, compensation resistor binding post; B, compensation resistors; C, strain gage sensing element; D, safety stop; E, diaphragm.

Figure 7. Sectional View of a Compensated and Standardized Strain-Gage Pressure Transducer

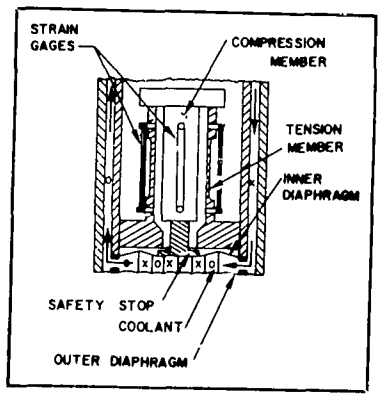


Figure 8. Sectional View of a Water-Cooled Pressure Tra

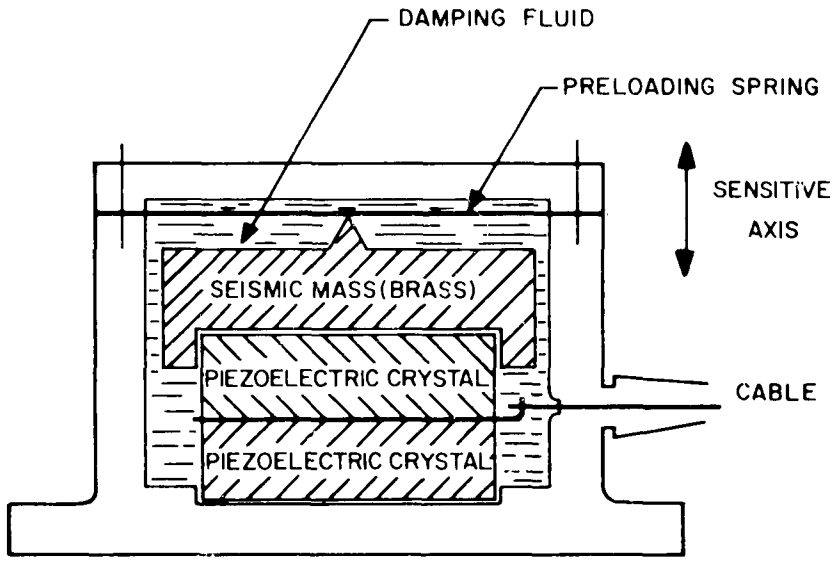


Figure 9. Cross-Section of Compression Type Crystal Accelerometer

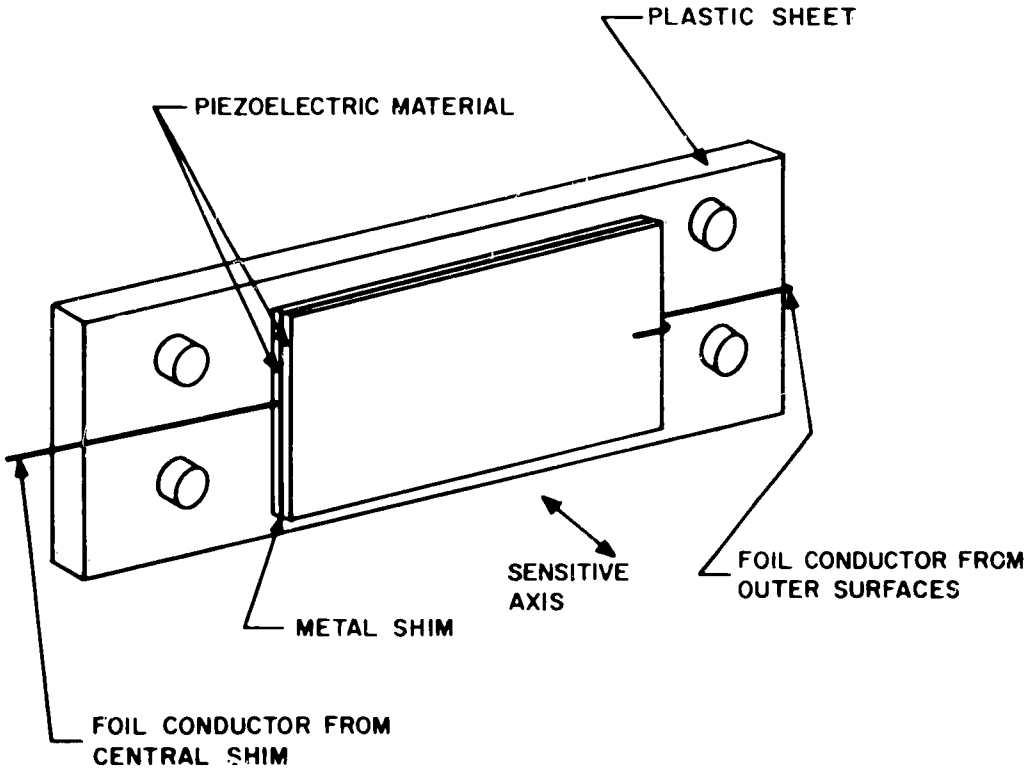


Figure 10. End Supported Bimorph Crystal Accelerometer

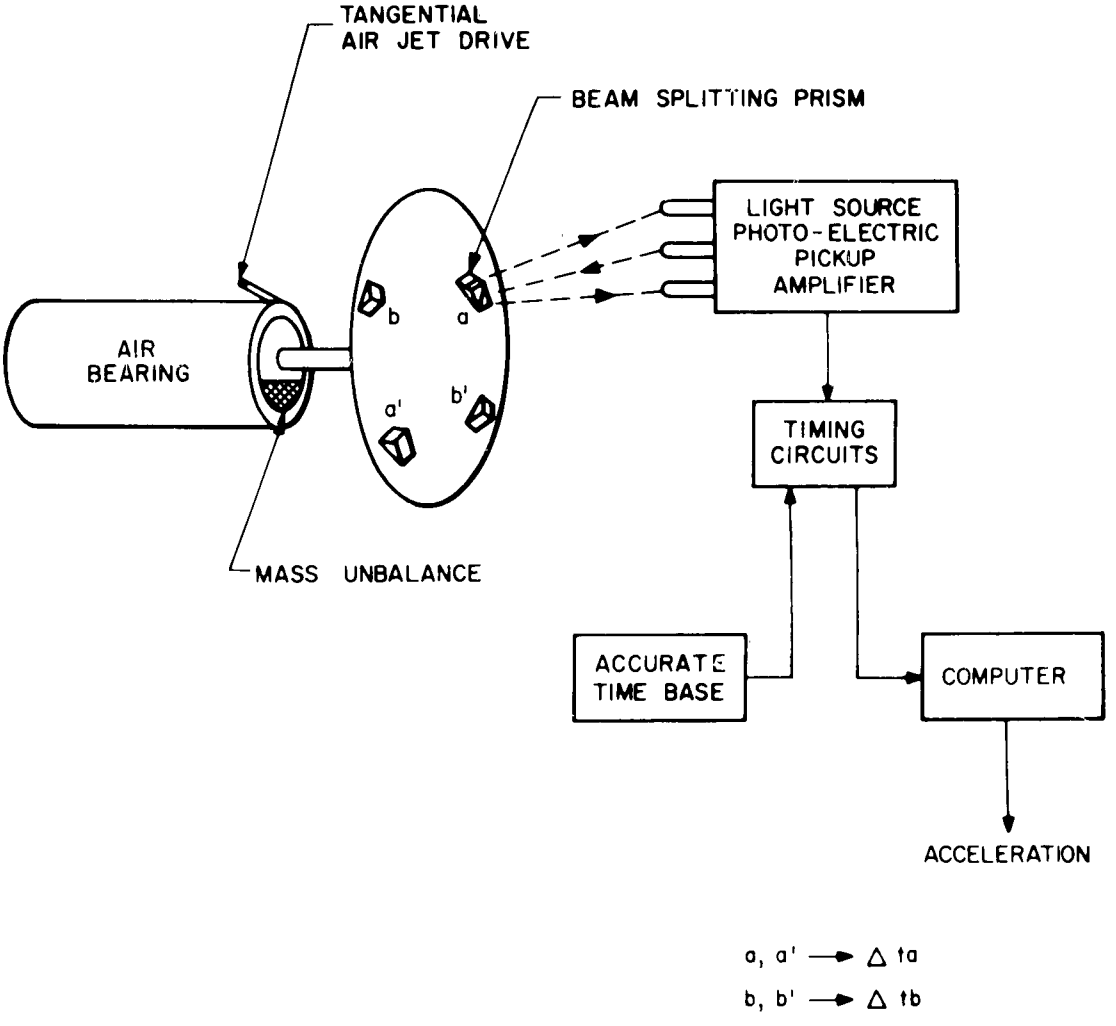


Figure 11. Block Diagram of Rotating Pendulum Accelerometer

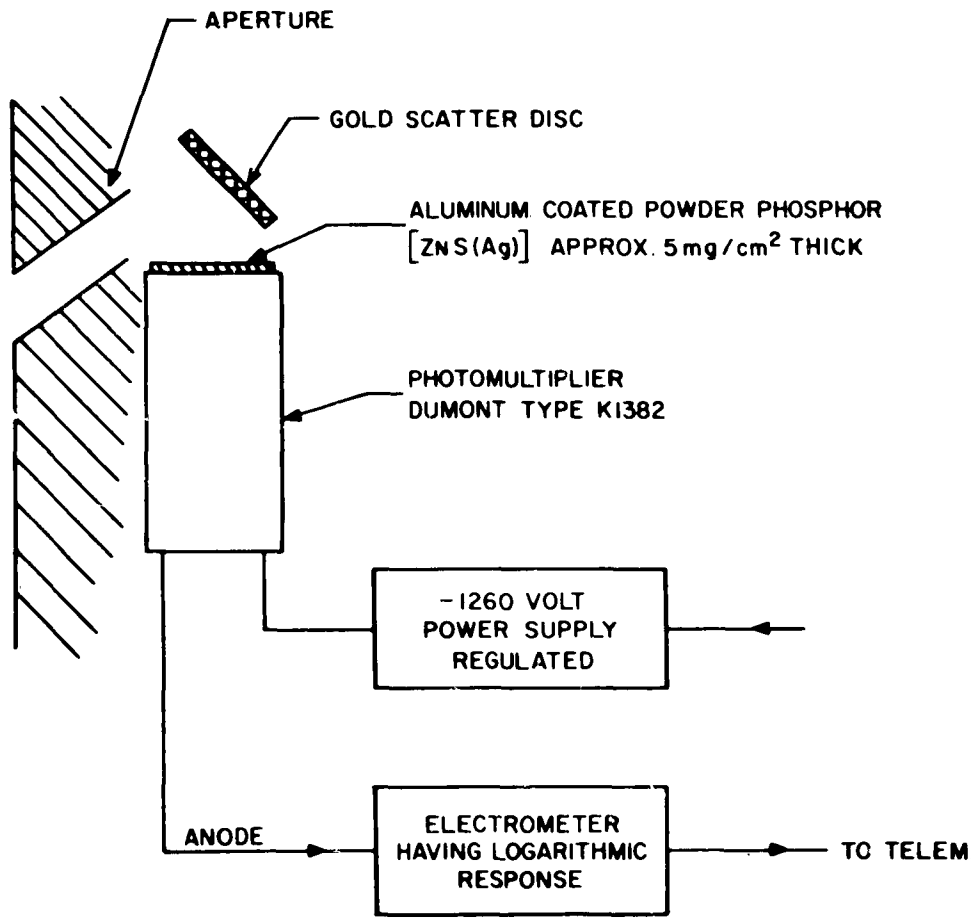


Figure 12. Electron Detector

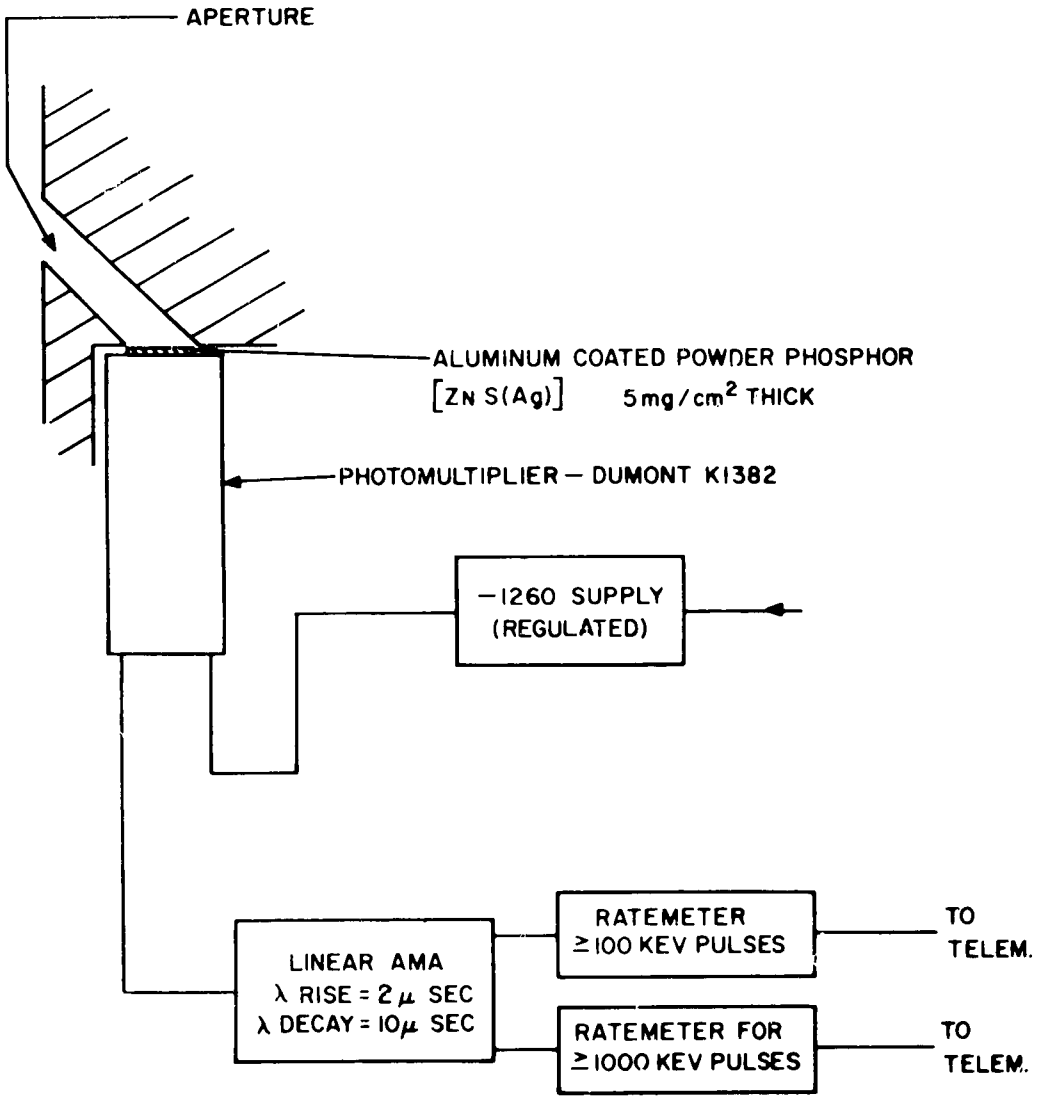


Figure 13. Ion Detector

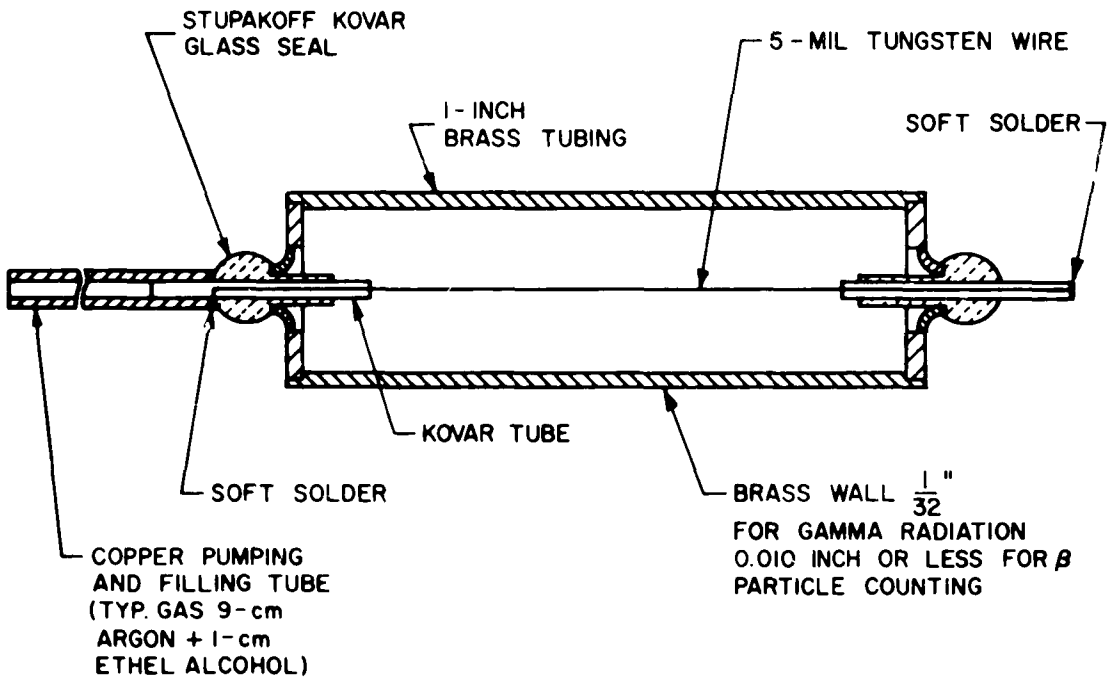


Figure 14. Typical Geiger - Mueller Counter

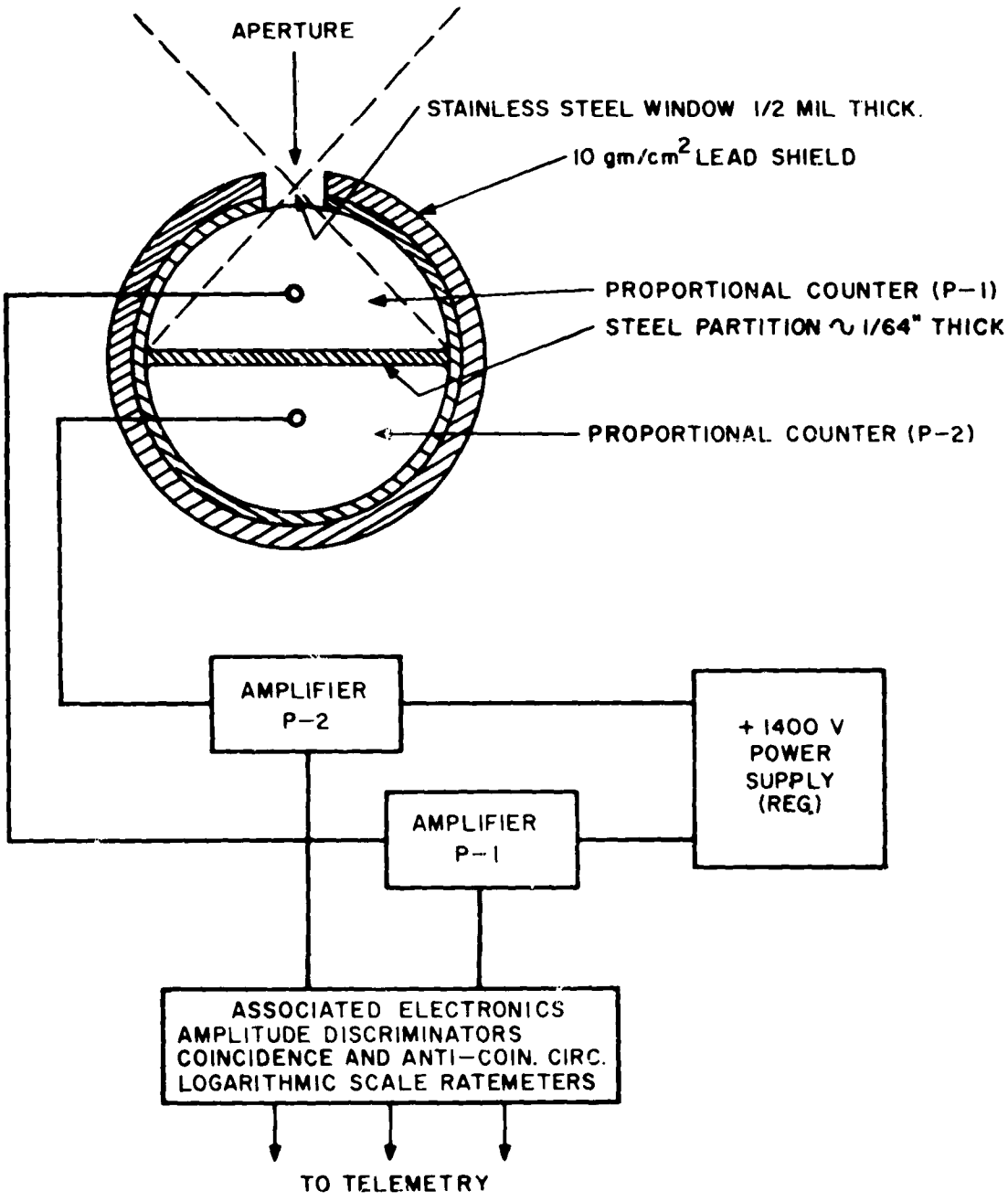


Figure 15. Proportional Counter Telescope

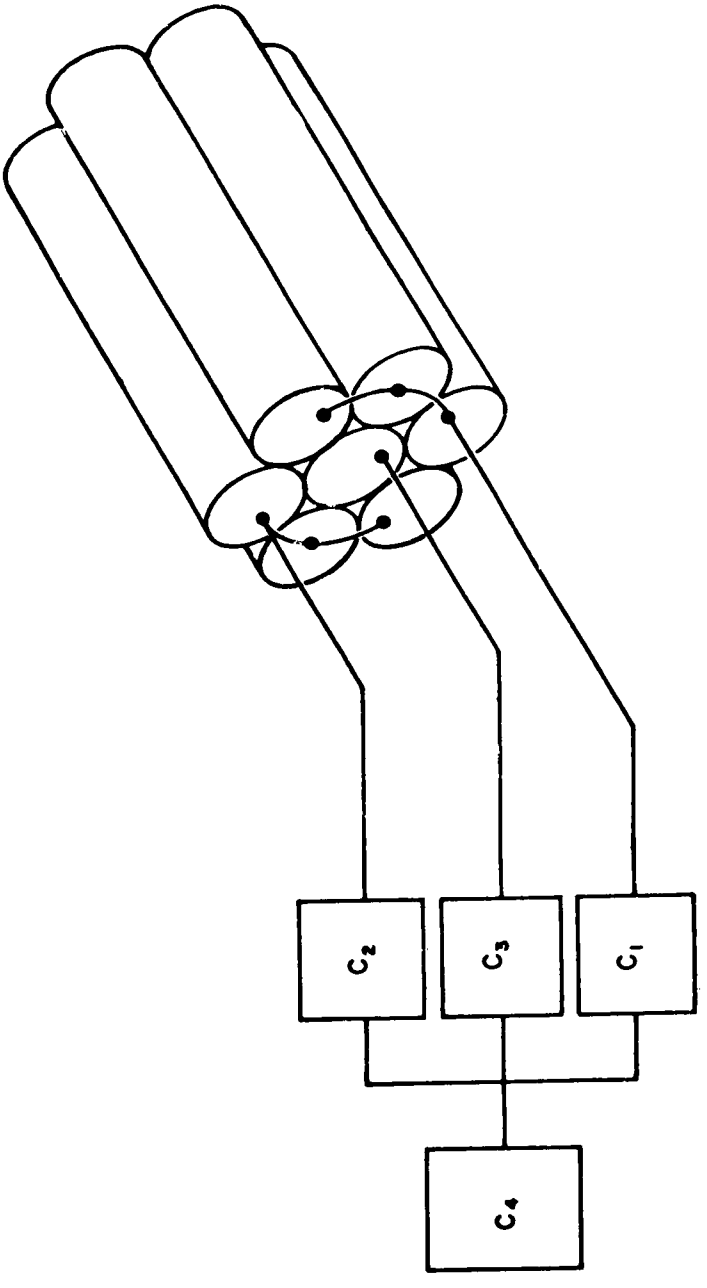


Figure 16. University of Chicago Proportional Counter Telescope

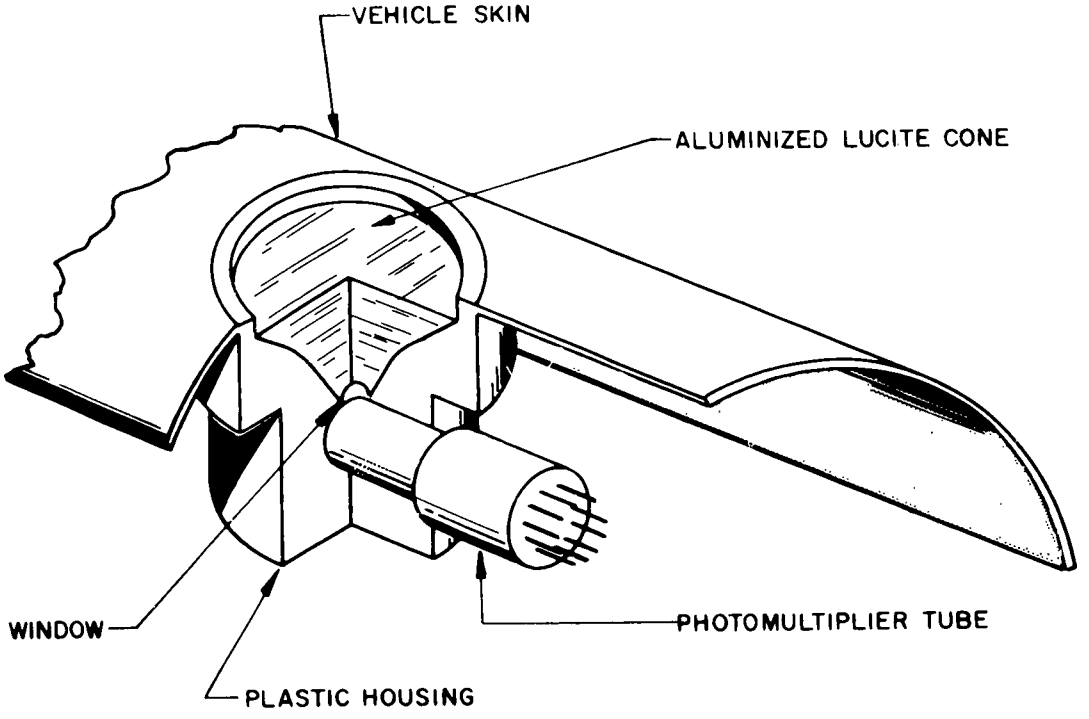


Figure 17. Cutaway View of Berg Scintillation Detector

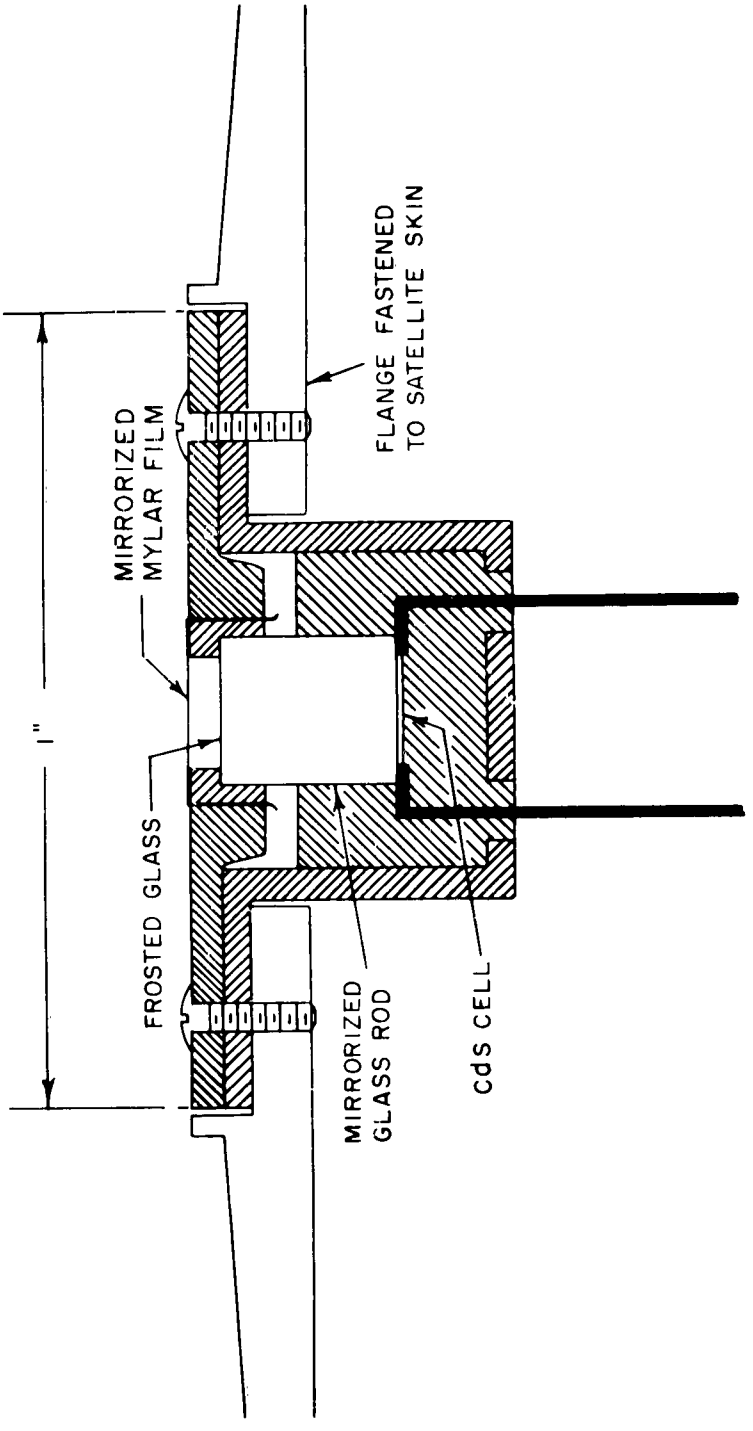


Figure 18. Photosensitive Micrometeorite Detector

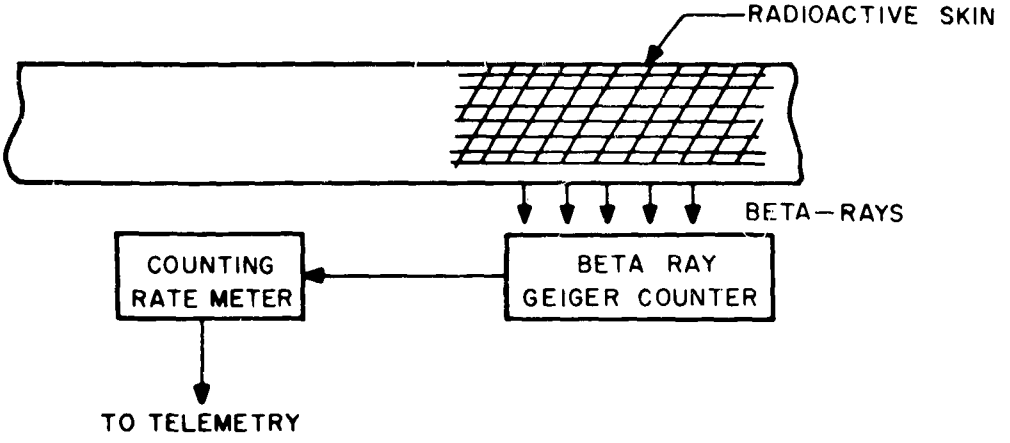


Figure 19. Radioactive Method (Singer)

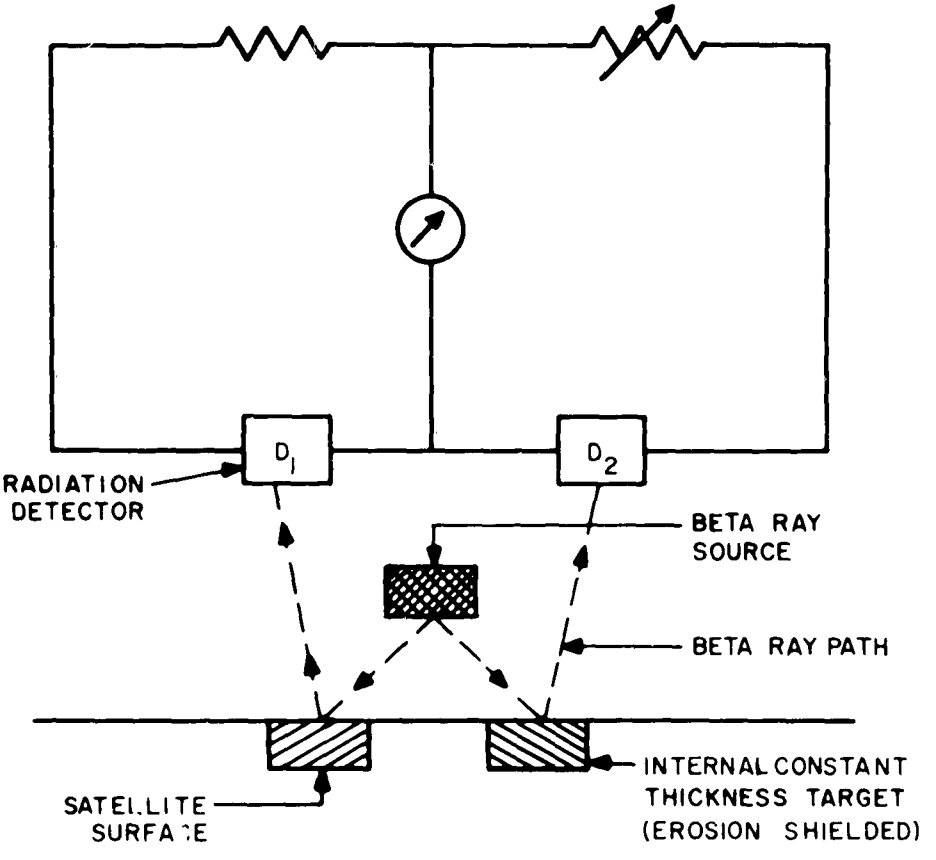


Figure 20. Circuit Arrangement for Increasing Sensitivity and Excluding Cosmic Background (Goettelman)

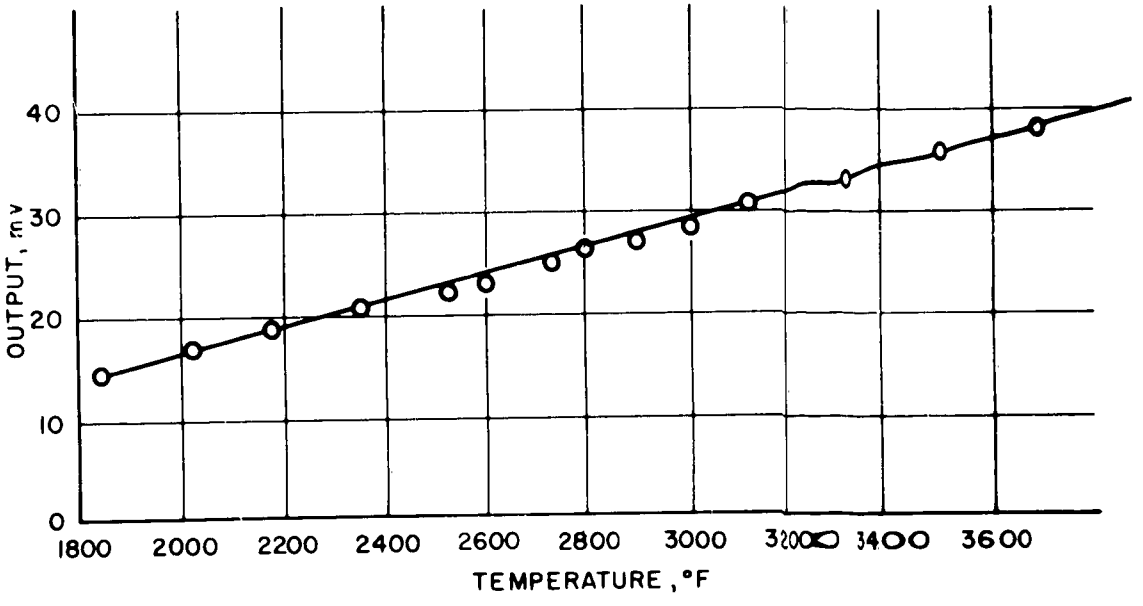


Figure 21. Tungsten - Iridium Thermocouple Output

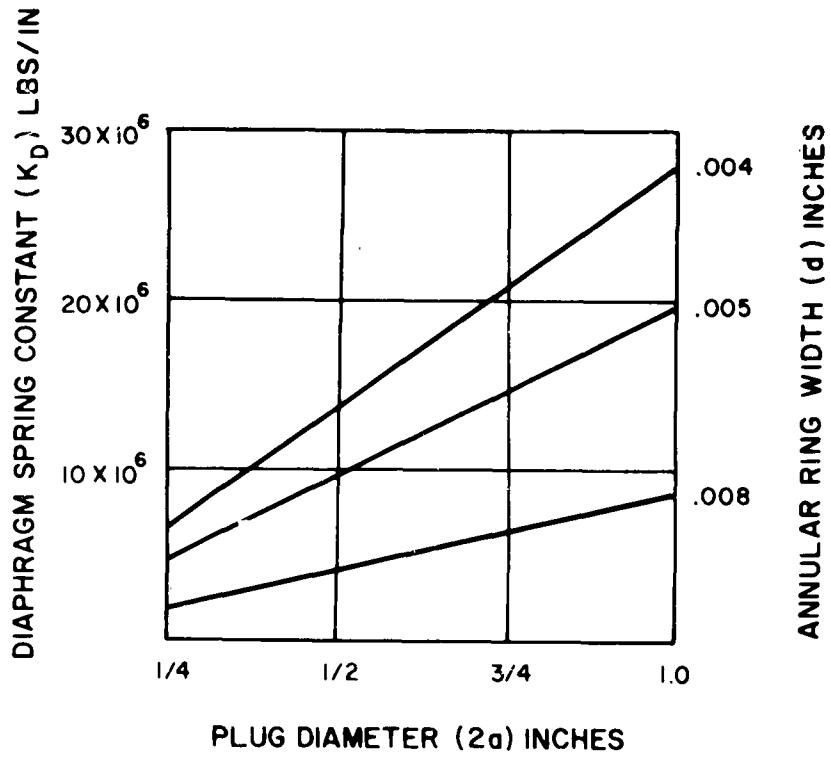


Figure 22. Plug Deflection Plotted Against Diameter for Several Ring Widths.

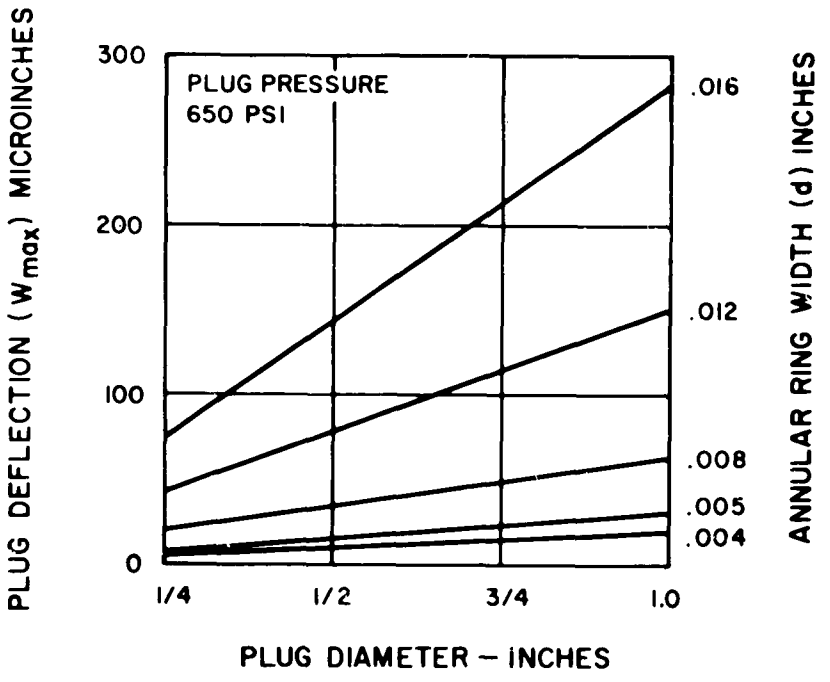


Figure 23. Equivalent Spring Constant for Various Combinations of Ring Width and Plug Diameter

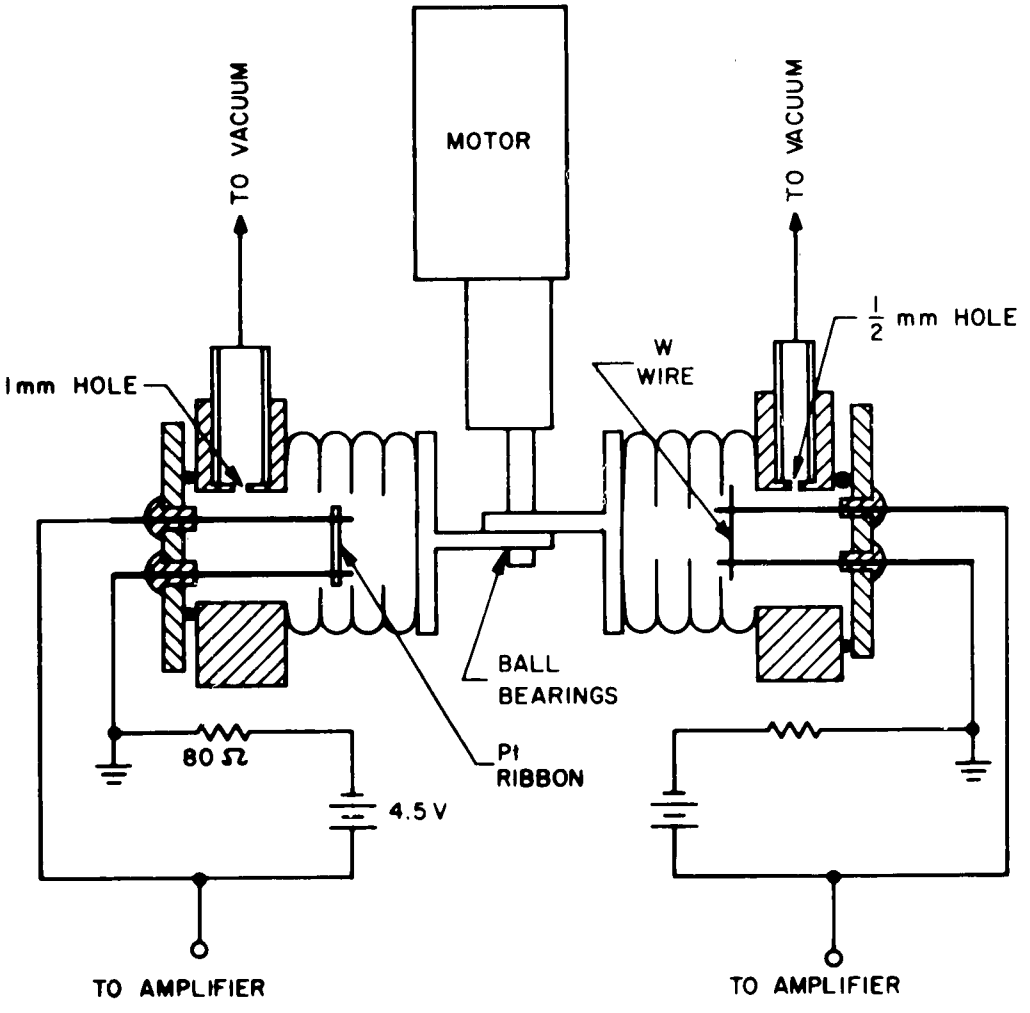


Figure 24. Schematic Drawing of Cyclic Vacuum Gage

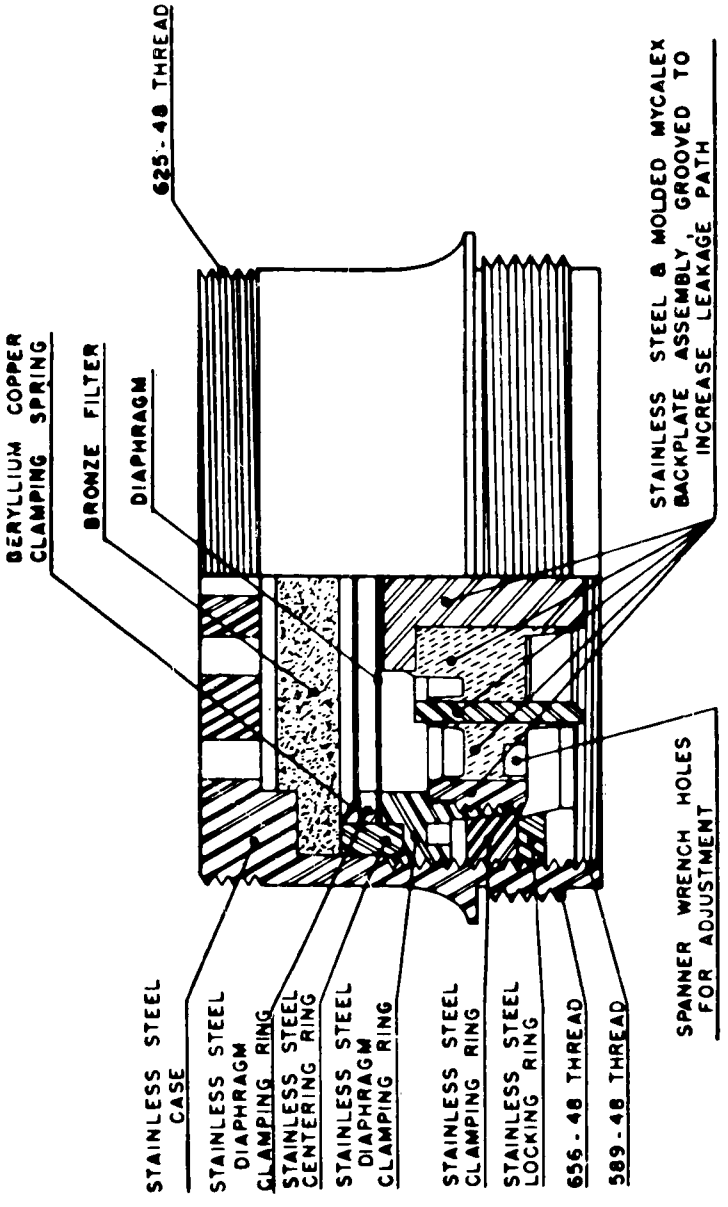


Figure 25. Condenser Microphone

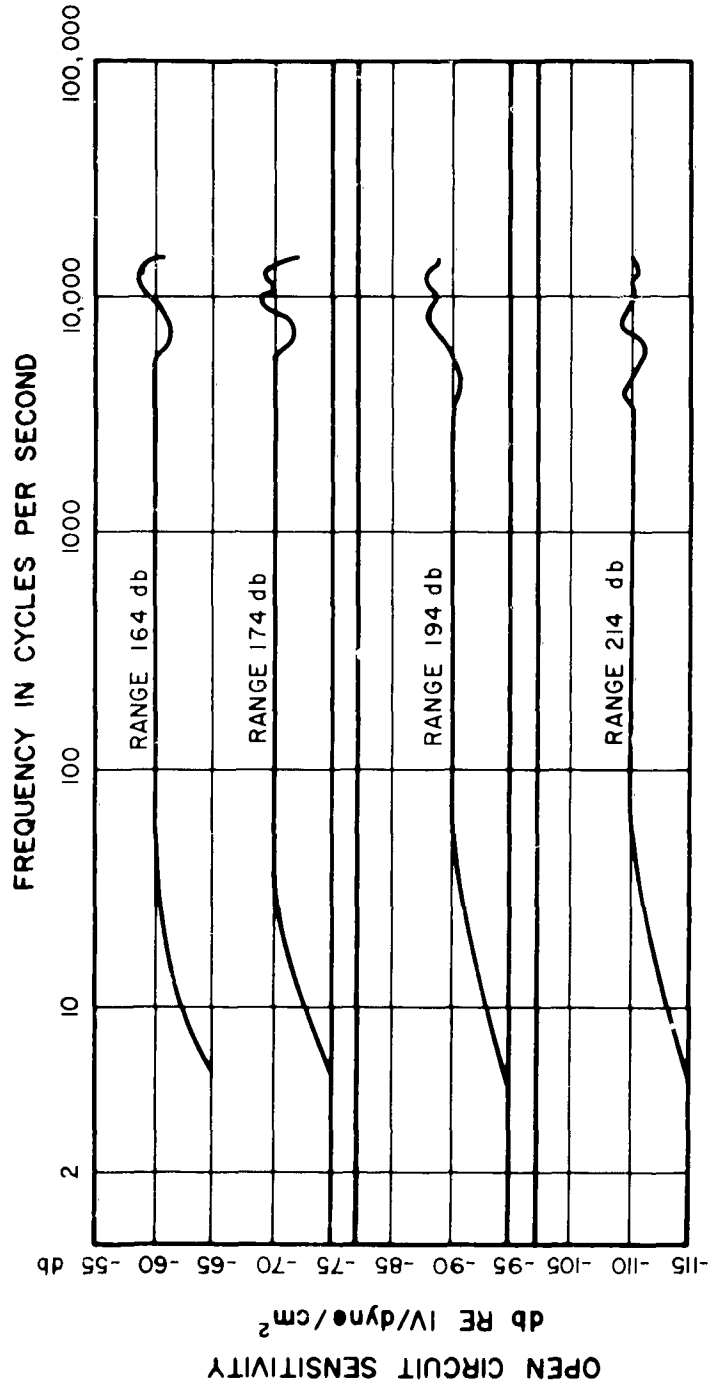


Figure 26. Typical Frequency Response Characteristics for Condenser Microphones

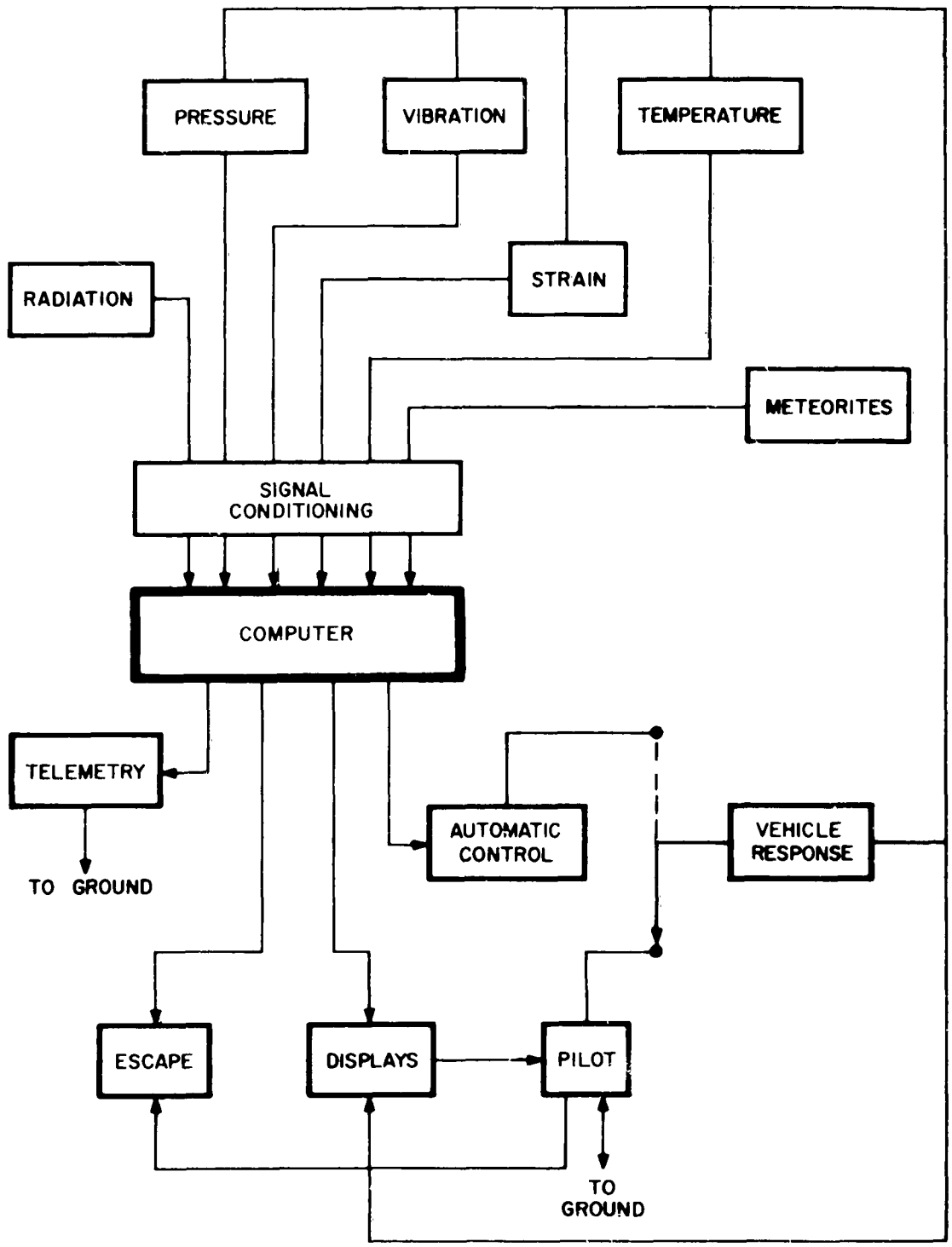


Figure 27. Simplified Block Diagram of Environmental Instrumentation

DISTRIBUTION LIST

| Cys | ACTIVITIES AT WPAFB |
|---|---|
| 20 | WWRCE-1<br>Attn: Paul Polishuk |
| 1 | WWAT |
| 1 | WWAD (Library) |
| 1 | WWDPFC-1<br>Attn: Mr. J. Long |
| 1 | WWDPFC-2<br>Attn: Mr. C. J. Jolley |
| 1 | WWRNRE-2<br>Attn: Mr. J. M. Francis |
| 5 | WWRMFE-2<br>Attn: Fred Sackleh |

OTHER DEPT. OF DEFENSE ACTIVITIES

| | |
|---|---|
| 1 | National Aeronautics and Space Administration<br>Attn: Mr. J. E. Jackson<br>Washington 25, D. C. |
| 1 | National Aeronautics and Space Administration<br>Attn: Mr. O. Berg<br>Washington 25, D. C. |
| 1 | National Aeronautics and Space Administration<br>Attn: Mr. L. Secretan<br>Washington 25, D. C. |
| 1 | National Aeronautics and Space Administration<br>Attn: Mr. L. Davis<br>Washington 25, D. C. |
| 1 | National Aeronautics and Space Administration<br>Attn: Mr. Ainsworth<br>Washington 25, D. C. |

| Cys | |
|---|---|
| 1 | National Aeronautics and Space Administration<br>Attn: Mr. J. R. Milligan<br>Washington 25, D. C. |
| 1 | Naval Research Laboratory<br>Attn: J. C. Holmes<br>Washington 25, D. C. |
| 1 | Staff Applications Officer<br>Programs Division<br>Attn: M. B. Gilbert<br>GRD, Air Force Cambridge Research Laboratories<br>Bedford, Mass. |

OTHER U. S. GOVERNMENT AGENCIES

| | |
|---|---|
| 25 | Armed Services Technical Information Agency<br>Arlington Hall Station<br>Arlington 12, Virginia |

NON-GOVERNMENT INDIVIDUALS AND ORGANIZATIONS

| | |
|---|---|
| 1 | Space Technology Laboratories<br>Attn: Dr. J. W. Lindner<br>P. O. Box 95001<br>Los Angeles 45, California |
| 1 | Space Technology Laboratories<br>Attn: Dr.Allen Rosen<br>P. O. Box 95001<br>Los Angeles, California |
| 1 | Jet Propulsion Laboratory<br>Attn: Dr. W. S. MacDonald<br>Space Sciences Section<br>4800 Oak Grove Drive<br>Pasadena, California |
| 1 | North American Aviation Company<br>Attn: Mr. Fred A. Payne<br>Chief, Preliminary Analysis<br>Los Angeles, California |



* U. S. GOVERNMENT PRINTING OFFICE : 1961 O - 608609